REVIEWS OF GEOPHYSICS AND SPACE PHYSICS, VOL. 11, NO. 3, PP. 513–570, AUGUST 1973

# Equatorial Undercurrent: Measurements and Theories

S. G. H. PHILANDER

*Geophysical Fluid Dynamics Program, Princeton University*
*Princeton, New Jersey 08540*

An eastward jet in the equatorial thermocline and, below it, a weaker westward current extending to a depth of about 1200 meters have been observed at practically all longitudes. In the western Pacific the flow in the deep (150 meter) mixed layer above the thermocline is westward at and near the surface and eastward at greater depths when the winds are westward. These shallow currents appear to reverse direction when the monsoons do. At longitudes where a deep mixed layer is absent, the Atlantic and eastern part of the Pacific, the undercurrent in the thermocline is symmetric about the equator, has its downstream flow in geostrophic balance, and is marked by deep penetration of warm water of high oxygen concentration when the winds are light. When the southeast trades gain in strength, the core of the undercurrent moves upwind, its zonal flow becomes ageostrophic, the westward surface flow becomes stronger, the subsurface eastward flow becomes weaker, the ridging of isotherms at the equator becomes more pronounced, and the troughing becomes less pronounced. The evidence in favor of these variations occurring systematically is very tenuous. For a constant-density model to be relevant to the motion observed in the mixed layer of the western Pacific, it must be nonlinear and the vertical diffusion of momentum must be important at all depths. The results of such models are in reasonable agreement with observations if the winds are westward. To explain the eastward flow in the thermocline below the mixed layer, a stratified model is necessary. According to one such model, density gradients, in the absence of local winds, give rise to an eastward surface current in the equatorial thermocline and below it to a westward current. The meridional circulation is marked by equatorial downwelling. The modification of these 'thermally' driven currents by local winds is consistent with the earlier description of the flow at longitudes where a mixed surface layer is absent.

## CONTENTS

## 1. INTRODUCTION

An intense, predominantly eastward, subsurface jet at the equator was discovered in the Atlantic in 1886 by *Buchanan* [1886, 1888]. *Puls* [1895], who was unaware of these measurements, noted that when the trades die out for a period of time, frequently in March and April, the surface flow at the equator is eastward. He also pointed out that the surface flow to the north of the equator in the region of the eastward North Equatorial Countercurrent is sometimes westward. Puls postulated that an eastward subsurface current may be present at all times, but it is unclear whether he was referring to the latitudes of the countercurrent only (*Stroup and Montgomery* [1963] believe this to be the case) or whether he was referring to the equator also (*Metcalf* [1963] believes he was). Japanese oceanographers who started measuring the flow in an eastward subsurface equatorial current in the western Pacific around 1925 were unaware of the earlier measurements and speculations. All these observations fell into oblivion until shortly after the rediscovery of the undercurrent in the Pacific in August 1952 by *Cromwell et al.* [1954], who suggested the name 'Equatorial Undercurrent.' For further historical details the reader is referred to an essay by *Matthäus* [1969].

There is at the moment some confusion as regards an appropriate name for the current. Shortly after Cromwell's death, *Knauss and King* [1958] proposed that the current be called the Cromwell Current. Subsequent to the first current-meter measurements of the undercurrent in the Atlantic Ocean from on board the R.V. *Mikhail Lomonosov,* the eastward subsurface equatorial current in that ocean basin has frequently been referred to as the Lomonosov Current. *Wooster* [1960] has noted that the name Equatorial Undercurrent is more consistent than either of these names with present practice in naming features of the oceanic circulation. However, *Rual* [1969] and *Rotschi and Wauthy* [1969] protest that to call the current a 'sous-courant' in French is to commit a solecism. Similar considerations must obtain in Russian, for *Burkov* [1966] suggests the name Deep Equatorial Countercurrent for a reversal of the equatorial flow at depth, reserving the shortened name Equatorial Countercurrent for a reversal of the (expected) westward flow in the same horizontal plane. In this paper an intense eastward jet in the vicinity of the thermocline at the equator will be referred to as an Equatorial Undercurrent. Note that this

current may have two cells, so that there are effectively two currents, and that it may on occasion surface, in which case it is no longer an undercurrent. We follow *Hisard and Rual* [1970] in naming the westward current below the eastward undercurrent the Intermediate Equatorial Current. This name derives from the location of this current in the intermediate water of the Pacific [*Reid*, 1965]. The westward flow above the undercurrent is usually part of the South Equatorial Current, which is flanked by the eastward North and South Equatorial Countercurrents. Figure 1 shows the relative positions of the various currents in the central Pacific. At other longitudes it is possible for the North Equatorial Countercurrent to be contiguous to the undercurrent (in the western Pacific, for example) or to have its southern edge south of the equator (in the Indian Ocean, for example).

A detailed review of measurements and theories of the Equatorial Undercurrent is presented in sections 2 and 3, respectively. New results are discussed in section 4. The remainder of section 1 is a summary of the measurements and main theoretical results and is intended for the reader who is interested only in a bird's-eye view of developments to date. The salient result to emerge is that the equatorial currents are variable and sensitive to changes in local wind conditions but that the data are insufficient to establish a correlation between changes in the wind conditions and variations in the structure of the currents. Though an expedition by a single oceanographic vessel for a short period of time will always be of immense value, it will become evident that certain aspects of both the theory and description of the equatorial current system call for measurements, oceanographic and meteorological, on a scale much larger than is possible with a single ship. It is hoped that the Garp (Global Atmo-

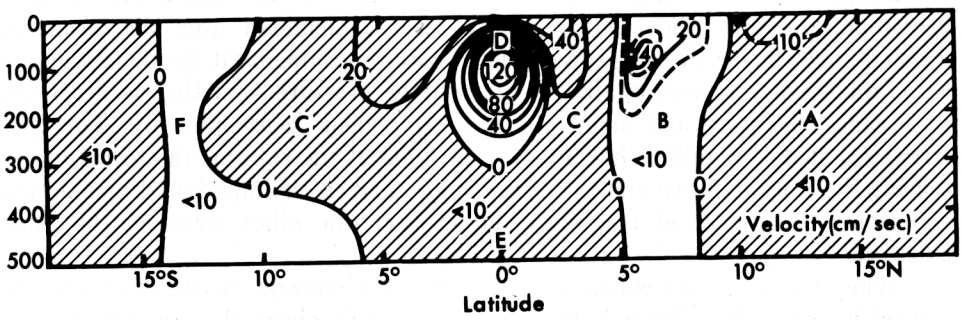


Fig. 1. Meridional cross section of the zonal component of the velocity (centimeters per second) in the central Pacific. Shaded regions indicate westward flow; unshaded regions indicate eastward flow. Velocities are geostrophic velocities except near the equator, where the values are based on direct observations [*Knauss*, 1960]. For the 'level of no motion,' 1000 meters was assumed. A, North Equatorial Current; B, North Equatorial Countercurrent; C, South Equatorial Current; D, Equatorial Undercurrent; E, Intermediate Equatorial Current; F, South Equatorial Countercurrent. (In principle, it is possible to compute equatorial currents from the measured density field [*Hidaka*, 1962], but the results are in general unreliable, since small errors in the measurements of the density field can lead to large errors in the calculated velocities. The currents measured by *Koshlyakov and Neyman* [1965], for example, have little in common with the currents they calculated from the density field.) [After *Knauss*, 1963.]

spheric Research Program) Atlantic Tropical Experiment (Gate) in the summer of 1974 will afford an opportunity for such measurements.

*a. Summary of the measurements.* Observed at practically all longitudes in the ocean are an eastward current in the equatorial thermocline and, below that, a westward current that can extend to depths in excess of 1200 meters. The eastward undercurrent has a half-width of approximately $1\frac{1}{2}°$ latitude and can attain speeds up to 170 cm/sec; speeds of 40 cm/sec have been recorded in the westward Intermediate Equatorial Current. There are measurements below 1500 meters in the Pacific only, and those indicate that the flow reverses once more, so that the very deep flow at the equator is eastward and remarkably steady over a period of months. The deep equatorial currents in the Atlantic are bound to be different, since the topography there is very irregular; the mid-Atlantic ridge runs along part of the equator, so that the depth of the ocean hardly exceeds 2000 meters in certain places.

In the eastern part of the Pacific and in the Atlantic Ocean, where there is usually no deep homogeneous surface layer at the equator, the eastward current in the thermocline is very sensitive to changes in local wind conditions. Although the number of observations to date is sufficient to establish the variability of the structure of this current (it may or may not be symmetric about the equator; it may or may not have its zonal flow in geostrophic balance; it may or may not be characterized by deep penetration of warm water), the data are not by any means sufficient for systematic variations in the structure to be discernible. It is, of course, possible to postulate systematic variations that are consistent with the available data. We shall now proceed to do so. It must be stressed that the evidence on which this description is based is very tenuous. In the description we shall refer to the zonal flow at the equator as being in geostrophic balance when the pressure fields as calculated from the measured density field (under the assumption that pressure gradients at depth are small) agree quantitatively and qualitatively with the pressure field that is necessary to balance the measured zonal velocity component geostrophically. For geostrophy it is also required that up to $\frac{1}{2}°$ latitude of the equator the terms representing the Coriolis force and the pressure gradient in the meridional momentum equation be an order of magnitude larger than the other terms in the same equation.

When the westward winds are weak, the undercurrent, at longitudes where a deep mixed surface layer is absent, is symmetric about the equator, has its downstream flow in geostrophic balance, and is marked by deep penetration of warm water of high oxygen concentration (see Figure 10 in section 2*b*). The upper isotherms and isopleths of oxygen concentration, however, ridge at the equator, so that there is usually a narrow belt of cold water of low oxygen content at the surface at the equator. If the winds should die out for a period of time, the surface flow is eastward rather than westward, a phenomenon referred to as the surfacing of the undercurrent. An increase in the intensity of the westward winds (the southeast trades gain in strength between April and August) causes the isotherms to ridge in a more pronounced manner and to trough in a less pronounced manner. Figure 2 gives an indication of the extent

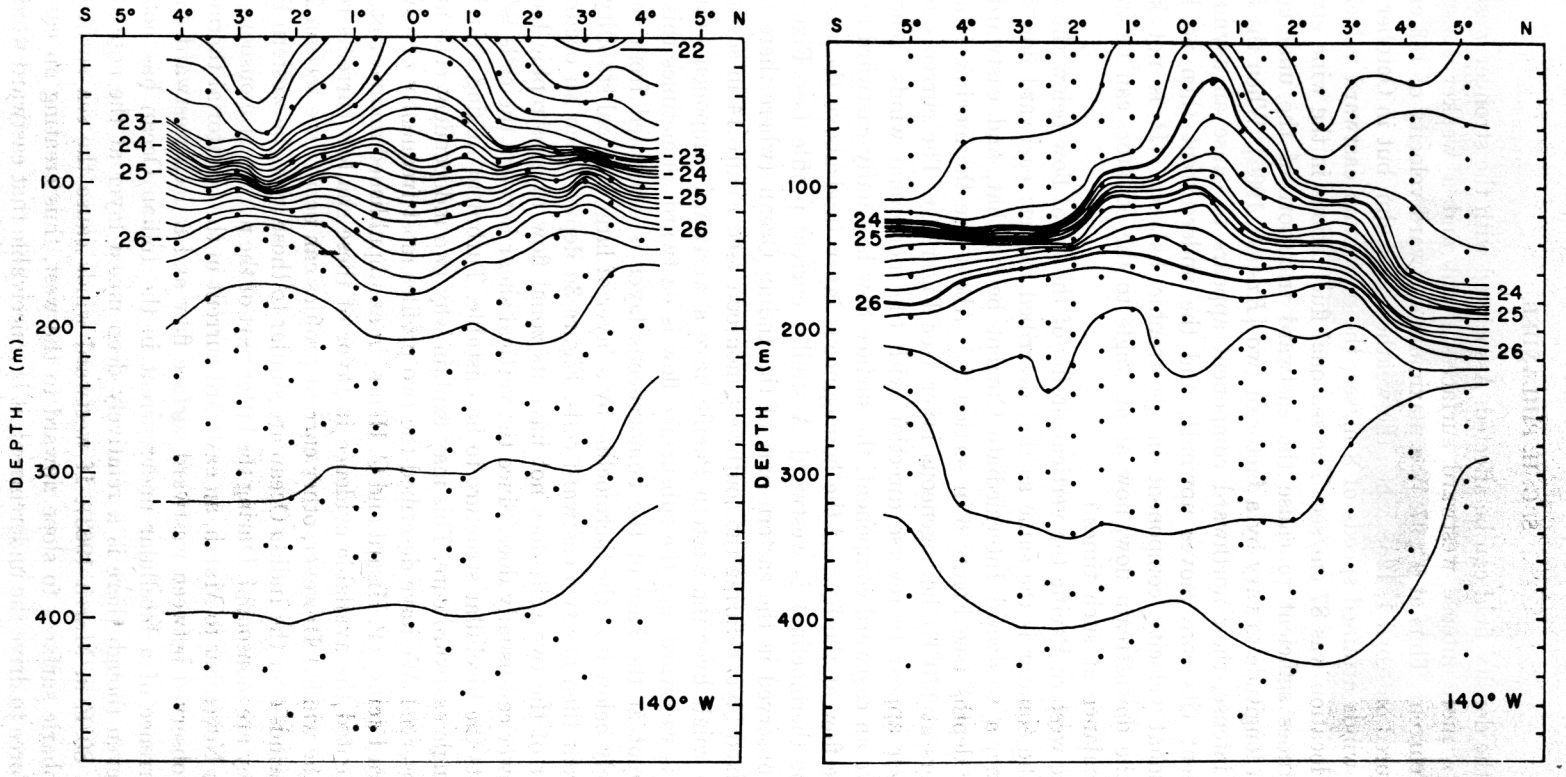


Fig. 2. Isopycnals (units of $\sigma_t$, g/l) in a meridional plane at 140°W as observed (left) in May 1958, when the winds were weak, and (right) in October 1961, when the southeast trades were intense. [After *Knauss*, 1966.]

to which the density field can be affected. Associated with the stronger westward winds is a more intense westward surface current and a weaker subsurface eastward current. Thus at 0°, 97°W a maximum eastward velocity of 143 cm/sec was measured on April 1, 1968, when the weather was calm, but in October 1961, when the winds attained speeds of 8 m/sec, the maximum eastward velocity at the same location was 87 cm/sec. The seasonal fluctuations in the wind strength are sometimes sufficient to cause the eastward transport of the undercurrent at a given longitude to vary by a factor of two [*Knauss*, 1966]. When the trades are very intense, their northward component appears to cause an asymmetric undercurrent (its core moves upwind), and the undercurrent then no longer has its zonal velocity component in geostrophic balance. (It is not known whether the downstream flow, now at an angle to the equator, can be in geostrophic balance at such times.)

In the western Pacific the vertical profile of the zonal flow below the mixed layer at the equator is the same as that described earlier: eastward flow in the thermocline, a westward Intermediate Current below that, and eastward flow at greater depths (see Figure 6 in section 2*a*). Above the thermocline is a deep (150 meters at 170°E) homogeneous layer (see Figure 3). The currents in this mixed layer appear to reverse direction with the monsoonal winds. When the winds have an eastward component, the surface flow is usually eastward and the subsurface flow at the base of the homogeneous layer (and above the eastward flow in the thermocline) is westward. A similar current profile (see Figure 3*b*) has been observed in the eastern part of the Indian Ocean (where there is also a deep mixed layer) during the southwest monsoon (see Figure 14 in section 2). When the winds over the western Pacific have a westward component, the surface flow is westward and the subsurface flow is eastward. Sometimes this eastward current at the base of the homogeneous layer is separated from the one immediately below it in the thermocline by a layer of large vertical stability. The undercurrent then has two eastward cells. Figure 3*a* depicts such an occurrence. The upper of the two cells does not have its zonal flow in geostrophic balance, but the lower cell usually does. Since the vertical shear between the cells is large, one expects the bicellular structure to be unstable. Turbulent mixing would then cause a single eastward core. This may explain why two independent cells are not always observed. We have described the two profiles most frequently observed in the western Pacific. (P. Hisard and C. Henin, in an unpublished manuscript, 1972, have presented the available evidence in favor of these shallow currents reversing with the winds.) However, other current profiles can occur (see section 2*a*).

The winds over the Indian Ocean are similar to those over the western Pacific in that they are monsoonal. During the latter part of the northeast monsoon, which lasts from November to March, an eastward current in the equatorial thermocline has been observed between westward surface flow and a deep westward current. The occurrence of a bicellular undercurrent in the Indian Ocean has not been reported even though there is a relatively deep mixed layer at the equator (75 meters at 80°E in March 1963). If westward winds cause the sea surface and deeper isobaric surfaces to slope upward to the west, thus creating an eastward pressure force to drive the undercurrent, it is conceivable that eastward winds will

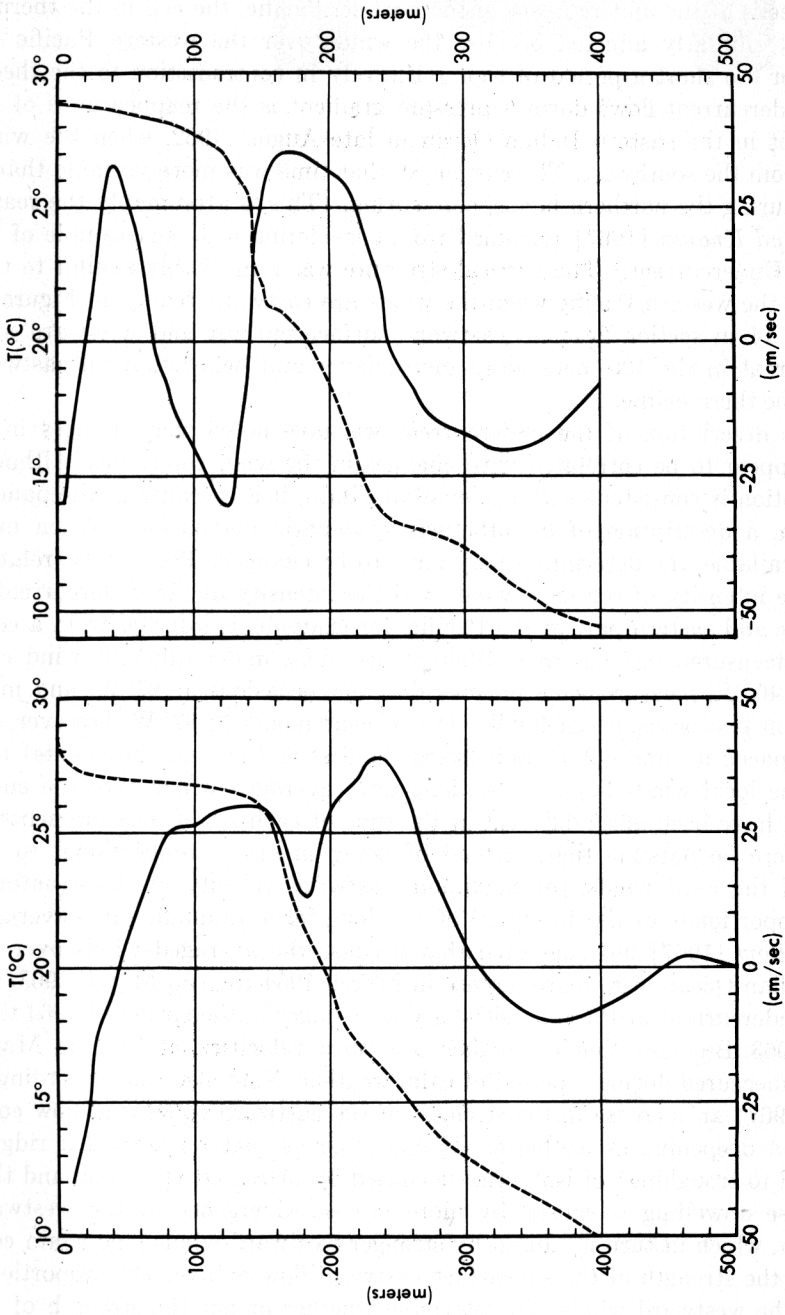


Fig. 3. The zonal velocity (solid lines) and temperature profile (broken lines) at 0°, 170°E as observed (left) in March 1967, when the winds were westward, and (right) in April 1967, when the winds were eastward. During the first half of April 1967, intense eastward winds prevailed, but at the actual time of the measurements shown on the right the winds were westward. [After *Hisard et al.*, 1970.]

destroy this source of momentum and perhaps the undercurrent. This appears to happen in the Indian Ocean, for after the onset of the southwest monsoon in May the undercurrent weakens, and by July it has apparently disappeared. (The lower of the two cells of the undercurrent in the western Pacific, the cell in the thermocline, is not similarly affected because the winds over the western Pacific are eastward for too short a period of time.) Entirely in contradiction to the theory that the undercurrent flows down a pressure gradient is the reappearance of the undercurrent in the eastern Indian Ocean in late August 1962, when the winds were still from the southwest. The current at that time was more variable than it usually is during the northern hemisphere spring. (This is presumably the reason why *Taft and Knauss* [1967] refrained from considering it as an example of the Equatorial Undercurrent.) The vertical structure was remarkably similar to that observed in the western Pacific when the winds are eastward (compare Figure 3*b* and Figure 14 in section 2*e*): an eastward surface current and westward subsurface current in the 100-meter-deep mixed layer and below that an eastward current in the thermocline.

In this description of the undercurrent we have noted that changes in its structure appear to be correlated with changes in the wind conditions. Although this description is consistent with the available data, it is, because of the paucity of the data, a description of hypothetical systematic fluctuations. When more data are available, the description may have to be changed. The inverse relation between the intensity of the local winds and the intensity of the undercurrent in the Atlantic and eastern part of the Pacific, for example, is inferred from a comparison of measurements on three different occasions under different wind conditions at 140°W, measurements on four different occasions at 97°W, and measurements on two occasions at 30°W. The measurements at 97°W, however, are so widely spaced in time (12 years between the first and last measurements) that not only the local winds but also the long-term averaged winds over the entire basin could have been quite different at the time of each set of measurements. It may therefore be possible that, instead of being inversely proportional to the intensity of the local winds, the maximum eastward velocity at the equator is directly proportional to the intensity of the long-term (annual, say) averaged winds. *Swallow* [1967] has suggested that because the averaged winds over the western Indian Ocean were more intense in March 1964 than in March 1963, the observed undercurrent at those longitudes was stronger in the spring of 1964 than in spring 1963. But note that the highest eastward velocities, at 58°E in March 1964, were measured during a period of calm weather. Note also that according to *Swallow* [1967] an increase in the strength of the eastward equatorial flow coincided with a deepening of isotherms. If one assumes that an increased ridging (as opposed to troughing) of isotherms is caused by increased upwelling and that more intense upwelling is caused by more intense divergence of the westward surface flow, which in turn is caused by stronger westward winds, one again concludes that the strength of the subsurface eastward flow is inversely proportional to that of the westward winds. To determine whether or not the strength of the undercurrent decreases as the westward winds increase, simultaneous wind and current measurements over a long period of time are necessary.

There is also a need for simultaneous measurements at different locations covering a large area. The undercurrent, in each of the ocean basins, derives a substantial part of its water from western boundary currents that flow equatorward. In the western Pacific, for example, the southward flowing Mindanao Current and a current along the northern coast of New Guinea feed the undercurrent. These two currents are in turn maintained by the westward flowing South and North Equatorial Currents. All the currents mentioned thus far are subject to considerable seasonal fluctuations. If data were available so that the equatorial current system could be considered as an entity, we might arrive at the conclusion that it is incorrect to correlate variations in the strength of the undercurrent with local wind conditions.

The discussion in the previous paragraphs underlines the very tenuous nature of the evidence on which is based the earlier description of the systematic variations in the structure of the undercurrent. The discussion also makes it evident that, for the purpose of clarifying the nature of these variations, an expedition by a single ship is of limited value. What is called for is a tropical oceanographic experiment on a spatial and time scale that is larger than would be possible with one vessel.

*b. Summary of the theories.* A perplexing number of theories have been proposed to explain the Equatorial Undercurrent. Many of these neglect density gradients. In such models, westward surface winds cause the sea surface to slope upward from east to west. The resultant eastward pressure gradient is, for certain parameter ranges but not for all (see section 3), sufficient to drive a subsurface eastward current below the westward surface flow. In addition to predicting a subsurface eastward equatorial current, the different models also manage to give the correct order of magnitude of at least some of the characteristic scales of the undercurrent. The scaling for the undercurrent must take into consideration that physical processes that are unimportant away from the equator cease to be negligible near the equator. Since several different processes become significant at about the same distance from the equator [*Robinson,* 1966], a model that includes only one of these processes will have at least the correct width for the undercurrent. The freedom to assign a convenient value to the coefficient of eddy viscosity, usually assumed constant (but see *Robinson* [1966]), facilitates the feat of predicting other scales correctly. A basis for deciding which of the constant-density models is pertinent to the motion observed in the well-mixed surface layer of the equatorial western Pacific is afforded by the condition that the parameter range of the model and that of the observed flow coincide. According to this criterion, only models that take into consideration the nonlinear advection of horizontal momentum and in which the vertical diffusion of momentum is important at all depths near the equator are relevant to the flow in the mixed surface layers. (If the vertical diffusion of momentum is important in a thin surface boundary layer only, the current in the homogeneous fluid cannot have a vertical shear.) Models that do not satisfy these conditions are of course valuable studies of the various types of motion possible between two concentric rotating spheres, a configuration which, as *Greenspan* [1968] pointed out, is interesting in its own right. A model that is relevant to motion in the homogeneous layer of

the western Pacific is that of *Charney* [1960]. In his model the nonlinear advection of momentum is crucial in maintaining the subsurface eastward flow in the presence of westward winds. These winds cause divergent westward surface flows with which upwelling is associated. To compensate, there is equatorward drift at the level of the core of the undercurrent. For a reasonable value (see section 3*a*) of the constant coefficient of vertical eddy viscosity, the profile of the zonal flow as calculated by *Charney* [1960] is in good agreement with the profile observed in the mixed layer of the western Pacific, provided the winds are westward. Earlier we raised questions concerning the appropriateness of correlating changes in the structure of the undercurrent with changes in local wind conditions. It is therefore of interest to point out that the flow in the equatorial boundary layer investigated by *Charney* [1960] depends on local wind conditions only. However, this is not true of the more diffuse boundary layer that surrounds the equatorial boundary layer and that effects a smooth transition to the extraequatorial flow [*Philander*, 1971*a*].

Observations show that the currents in the homogeneous surface layers of the western Pacific reverse direction with the winds (P. Hisard and C. Henin, unpublished paper, 1972). *Charney*'s [1960] numerical iterations diverge when the wind is eastward unless the flow is linear. (The same happens when the wind is westward, provided the Rossby number is large.) As the Rossby number increases, the fields develop cusps at the equator (see Figure 4), and at a certain stage the latitudinal derivatives at the equator become infinite. The inclusion of lateral friction in the model remedies this defect [*McKee*, 1973]. The behavior of the model when the surface winds are eastward has not been fully explored, and an explanation for the reversal of the currents in the homogeneous surface layer of the western Pacific has yet to be offered.

Constant-density models do not explain the permanent eastward flow observed in the thermocline below the mixed layer of the western Pacific. Since both the

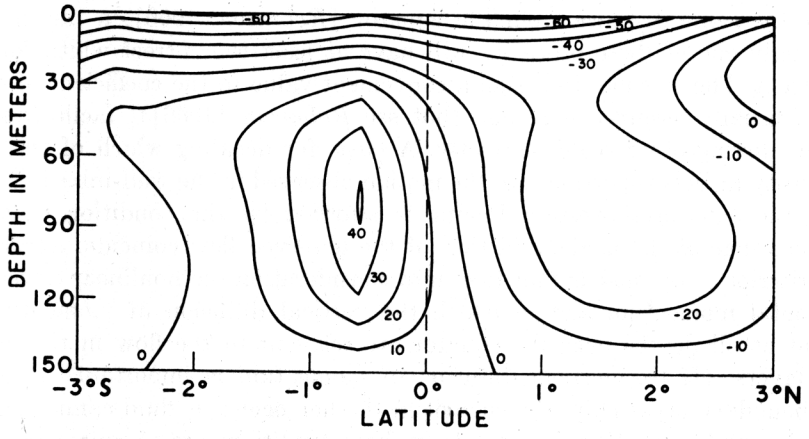


Fig. 4. A meridional section of the zonal flow (in centimeters per second) as given by a constant-density model without lateral friction when the magnitudes of both the northward and westward components of the wind stress are 0.45 dyne/cm². [After *Charney and Spiegel*, 1971.]

mixed layer and the upper cell of the undercurrent disappear as one moves eastward from the western to the central Pacific (see Figure 7 in section 2), the single-celled undercurrent in the thermocline of the eastern part of the Pacific is an extension of the undercurrent in the thermocline of the western Pacific. This current is again a consequence of the surface winds. *Montgomery and Palmén* [1940] originally proposed that the easterly trades blow water of low density westward, causing isotherms to slope upward from west to east as observed. If the pressure gradients at depth are assumed to be small, the density gradients associated with the sloping isotherms imply an eastward pressure force in the thermocline. This force is presumably the source of eastward momentum for the undercurrent. The slope of the isotherms reflects the long-term effect of the winds; if the winds were to abate for a short period of time, the density gradients would be modified but would not disappear. It follows that constant-density models can simulate the long-term effect of the winds in a crude manner by having an eastward pressure force but that a stratified model is necessary to accommodate both the short- and long-term effects of the winds.

Consider the motion due to density gradients in the tropics when the winds have temporarily died out. The upward (from west to east) slope of the isotherms shown in Figure 7 occurs not only at the equator but throughout the tropics. There is consequently an eastward pressure force near the surface throughout the tropics. Away from the equator and in the northern hemisphere the geostrophic current associated with this pressure force is southward (if velocities at depth are assumed to be small). In the southern hemisphere the corresponding current is northward. (*Knauss* [1966] has inferred such a flow south of the equator in the Pacific from the salinity distribution.) The fluid in the thermocline thus converges on the equator. At the equator, where the eastward pressure force cannot be balanced by the Coriolis force, the convergent fluid gives rise to an eastward current in the equatorial thermocline. A scale analysis shows that the width, depth, and downstream velocity of this current are comparable to the width, depth, and downstream velocity of the observed undercurrent. We thus have an explanation for the surfacing of the Equatorial Undercurrent in the eastern part of the Pacific and in the Atlantic during periods of calm weather. We can also account for the eastward current in the thermocline below the mixed surface layer of the western Pacific. On solving the equations describing this current, one finds that the zonal velocity reverses at depth [*Philander*, 1973]. A deep westward current beneath the eastward undercurrent has indeed been observed. A striking feature of the meridional circulation in the model is the occurrence of downwelling at the equator. This downwelling may be the explanation for the equatorial troughing of isotherms and for the deep penetration of water rich in oxygen at the equator (see Figure 10 in section 2*b*).

In the double-celled undercurrent in the western Pacific the upper cell is presumably a consequence of the local winds, whereas the lower cell is driven by density gradients in the manner just described. The observations that show that the upper cell does not have its downstream flow in geostrophic balance but that the lower cell does are consistent with this view. A profile such as that depicted in Figure 3*a* can arise in the following manner. After a spell of westerly winds

there will be eastward surface flow and westward subsurface flow in the mixed layer. If the wind direction should now change so that easterlies prevail, the surface flow will be affected immediately; the flow at greater depths will be affected somewhat later. The initial profile will therefore resemble the profile in Figure 3*b*, which may be regarded as an extreme case of a bicellular eastward undercurrent. If the easterlies should persist, the profile in Figure 3*b* will be transformed into the profile in Figure 3*a*. This process will be gradual if a layer of large vertical stability is present below the mixed layer, because such a sharp thermocline would tend to inhibit the vertical transfer of momentum [*Charney*, 1960]. Ultimately a subsurface eastward current with a single core will result unless the wind changes direction again. According to this theory, a bicellular undercurrent can occur in a region where a deep mixed layer is bounded below by a sharp thermocline, provided the winds over this region reverse direction occasionally.

In this paper (section 4) we investigate the manner in which 'local' winds modify the structure of the 'thermally' driven undercurrent at longitudes where there is no deep mixed layer. The effect of the local winds is incorporated by means of the surface stress boundary conditions. By keeping the longitudinal gradient of the sea surface temperature the same for all the cases to be discussed, the long-term effects of the winds will be kept unchanged. It will be shown that westward winds cause divergent westward surface flow that increases in intensity as the winds become stronger. The intensity of the (now) subsurface eastward current is inversely proportional to the intensity of the westward winds, so that the maximum eastward velocity decreases as the winds become stronger. Upwelling is associated with the divergent surface flow, and this, in conjunction with the downwelling at the core of the undercurrent, causes an equatorial spreading of the thermocline. As the westward winds grow in intensity, the downwelling becomes weaker, so that the isotherms trough less. For a sufficiently intense westward wind the thermocline could presumably spread upward only. Winds at an angle to the equator are found to cause an upwind displacement of the core of the undercurrent. Thus a wind with a northward component causes the core of the undercurrent to shift southward. This is true both in homogeneous (see Figure 4) and in stratified models. In the stratified model a wind with a northward component results in a region of convergence and a belt of intense downwelling north of the equator. This front moves farther northward as the southerly component of the wind increases in intensity. Experiments in which the northward component of the wind is zero but in which the westward component has a horizontal shear, so that the wind south of the equator is more intense than the wind north of the equator, show an undercurrent that is better developed in the northern hemisphere than in the southern hemisphere. It would appear that the proximity of the intertropical convergence zone (ITCZ) to the equator could affect the location of the core of the undercurrent.

The results of the model are entirely consistent with the observations to date. It does not follow that the model is adequate. The assumption that the coefficients of eddy viscosity are constant is of dubious merit. Because explicit zonal variations have been removed from the equations of motion by a similarity trans-

formation, only a small subset of the possible solutions to the problem can be obtained with this model. The similarity transformation also makes it impossible to answer questions concerning the origin and fate of the waters of the Equatorial Undercurrent. To remove these limitations, a genuinely three-dimensional model must be constructed. But even if such a model were to give results that are consistent with observations, it still would not follow that the physical processes that determine the structure of the undercurrent are adequately represented in the model. The possible importance of interaction with equatorial waves has been neglected (see section 5). To determine whether or not the model is adequate, it is necessary that the surface winds and sea surface temperature be given as input and that the model be used to simulate the flow observed under those conditions rather than idealized conditions. Once again we conclude that what is called for is an observational program on a scale larger than would be possible with a single ship.

## 2. MEASUREMENTS AND LABORATORY EXPERIMENTS

This section is a review of measurements of the undercurrent in the various ocean basins and of laboratory and numerical experiments that shed light on equatorial dynamics. It will become clear that the structure of the undercurrent is very sensitive to local wind conditions (unless the undercurrent is in the thermocline below a deep homogeneous surface layer). The winds depicted in Figure 5 therefore serve only as a rough guide to the type of wind variations that can cause some of the very low frequency changes to be discussed.

In an effort to learn something about the origin and fate of the water in the Equatorial Undercurrent, there have been several analyses of the changes in temperature, salinity, and oxygen concentration, among others, on isanosteric (constant potential density) surfaces. These surfaces are important when the diffusion of heat is negligible compared with the advection of heat, for in such an event fluid particles move on surfaces of constant density. If this were true it would be possible, for example, to infer that the origin of a belt of water of high oxygen concentration all along the equator on the 160 cl/t (centiliter per metric ton) surface in the Pacific is the Coral Sea, where there is water of the same oxygen concentration on the same surface [*Tsuchiya*, 1968]. This particular inference is questionable; according to *Hisard and Rual* [1970], eastward flow has been observed as often as westward flow on the 160 cl/t surface in the equatorial Pacific [*Hisard and Rual*, 1970, Figure 1]. The explanation for the inconsistency may be the following. The assumptions that imply that fluid particles move on constant-density surfaces are probably justifiable in nonsingular regions away from coasts but are unlikely to be valid near the equator. The equatorial region (within 2° latitude of the equator, say) by all indications is a singular region where there appears to be intense vertical mixing and strong vertical motion, both up and down. Consequently, a fluid particle at the equator is as likely to come from a location several thousand kilometers away in a horizontal direction as it is likely to come from a location a few hundred meters away in a vertical direction if both locations have the same oxygen concentration as the particle

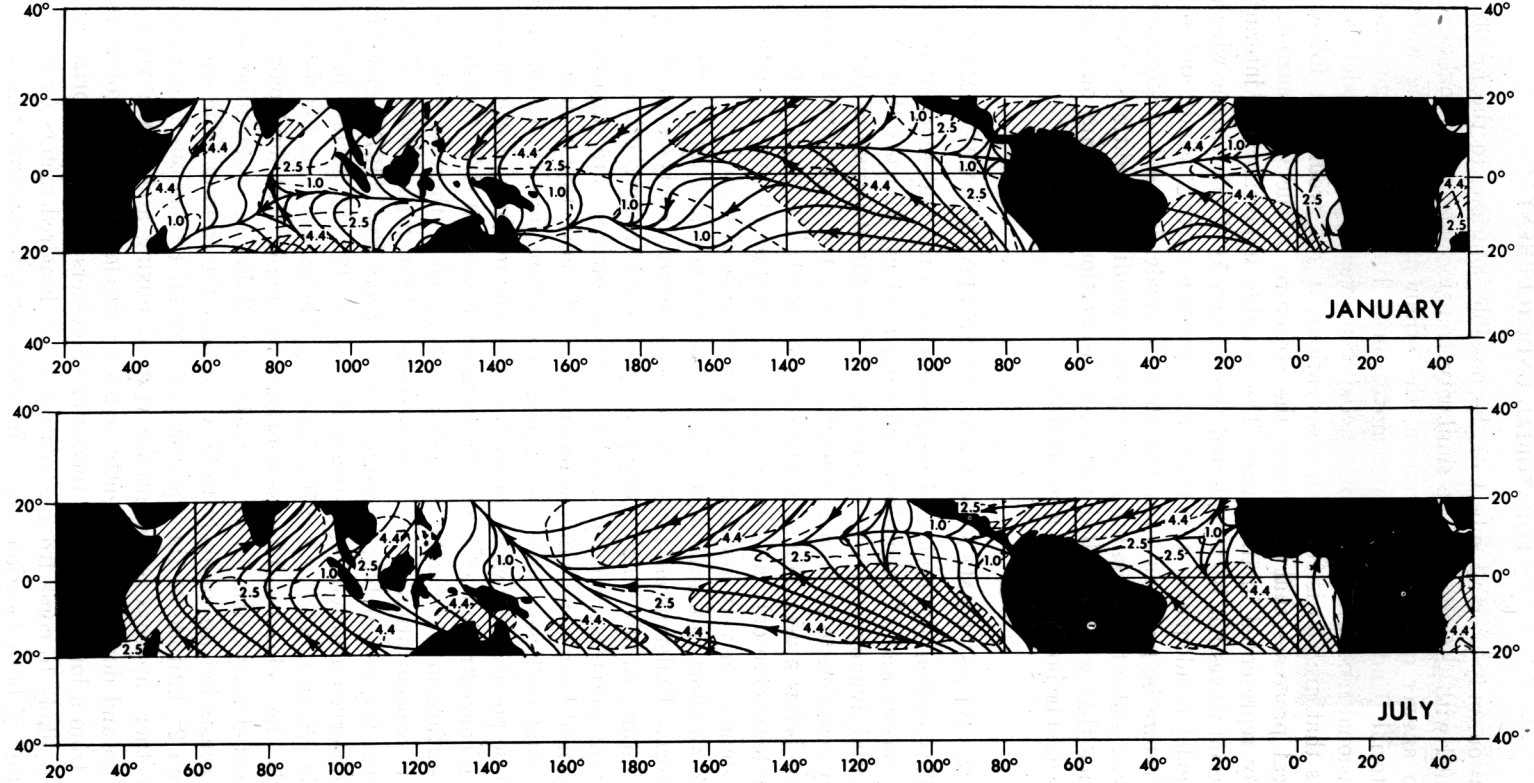


Fig. 5. The direction (solid lines) and intensity in meters per second (broken lines) of the winds in the tropics. In shaded regions the wind speed exceeds 4.4 m/sec. [After *Mintz and Dean*, 1952.]

and if oxygen is treated as a tracer. Caution must thus be exercised when interpreting the results of an analysis of water properties on constant-density surfaces.

In this paper the sverdrup is used as a unit of transport (1 Sv = $10^6$ $m^3$/sec); seasons referred to are northern hemisphere seasons.

*a. The western Pacific.* We follow *Montgomery* [1962] and denote the region from New Guinea (131°E at the equator) to the Gilbert Islands (174°E) as the western Pacific. This region differs from the rest of the Pacific in having monsoons: during the summer (July and August) the southeast trades cross the equator; in winter (around February) the winds are usually northeasterlies north of the equator but can have an eastward component at the equator. A further reason for isolating these longitudes is the possibility that the Gilbert Islands form a partial obstruction to the equatorial currents. This is, at the moment, only a possibility; with the exception of the identification of the undercurrent between the Gilbert Islands at 173°E [*Stroup and Hunt,* 1963] their effect on the current-countercurrent system has not yet been investigated.

The Equatorial Undercurrent in the Pacific is a permanent feature at longitudes east of 137°E. West of this longitude, eastward flow is regularly observed north of 2°N, but at the equator a subsurface eastward current is an intermittent phenomenon. The variable eastward equatorial flow west of 137°E can be viewed either as the undercurrent in its formative stages or as the North Equatorial Countercurrent; the two are joined by a continuous band of eastward flowing water in the western Pacific. One source for this eastward flow is the Mindanao Current, which is 50 km wide, is southward flowing, attains speeds up to 158 cm/sec, and has a transport in the vicinity of 28 Sv; it receives its water from the North Equatorial Current [*Masuzawa,* 1969; *Akamatsu and Sawara,* 1969; *Bogdanov and Popov,* 1960]. Another source for the eastward equatorial flow is the current along the northern coast of New Guinea. This coastal current approaches the equator rapidly west of 137°E, and its variability is the reason why eastward flow is observed only sporadically at the equator west of 137°E. During the summer the New Guinea coastal current is part of the westward-flowing South Equatorial Current. One would not be surprised to find that it reverses its direction in winter (when the winds have an eastward component), but measurements in November 1958 and December 1961 [*Yamanaka et al.,* 1965] and in the winters from 1967 to 1970 [*Masuzawa,* 1967, 1968; *Akamatsu and Sawara,* 1969; *Masuzawa et al.,* 1970] indicate that only the surface waters near the coast of New Guinea sometimes move eastward, whereas the subsurface flow is usually westward. One concludes that the flow south of 2°N and west of 137°E is not consistently eastward.

It is apparent from Figure 6 that the vertical structure of the zonal flow in the equatorial plane between 132°E and 152°E is most complicated. The only other longitude at which there are velocity measurements to similar depths is 170°E. In April 1967, when the winds had an eastward component, *Hisard et al.* [1970] observed eastward surface flow and westward subsurface flow in the deep (150 meter) homogeneous surface layer. In the thermocline below the well-mixed layer, Hisard et al. observed eastward flow, and below that westward flow (see Figure 3); the use of current meters from a drifting ship necessitated the assump-

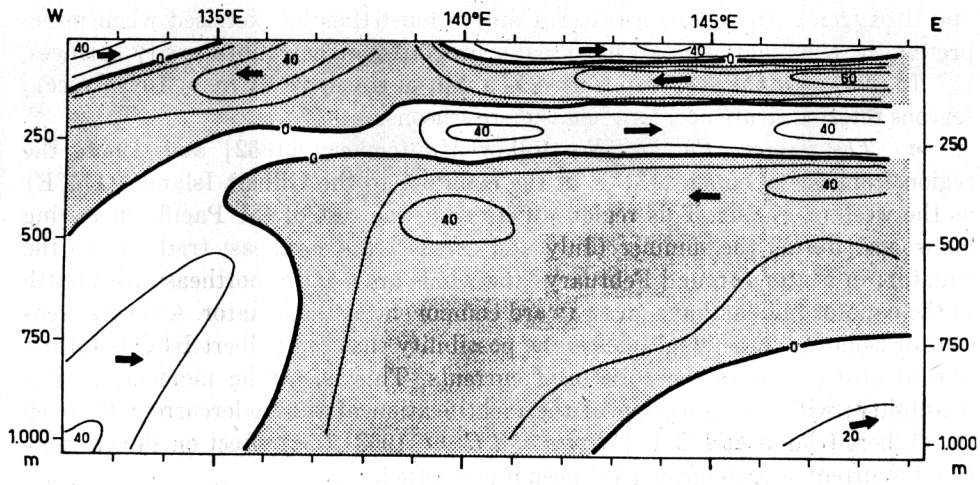


Fig. 6. Vertical structure of the zonal flow (centimeters per second) in an equatorial plane in the western Pacific, January–April 1966. [After *Kort et al.*, 1966.]

tion that the 500-meter depth is a level of no motion. *Rual* [1969] measured the shear of the current between 1000 and 1500 meters (1500 meters was assumed to be a level of no motion) at the same longitude and found that the deep westward flow observed by *Hisard et al.* [1970] extends to a depth of 1200 meters, with eastward flow below that. Because these are shear measurements, there is uncertainty about the direction of the flow at a given depth. Note, however, that the profile of the zonal flow at the equator from the surface to 1500 meters at 170°E in April 1967 is similar to the flow measured by *Kort et al.* [1966] with current meters on moored buoys (see Figure 6). The vertical structure of the flow from the thermocline downward is also similar to that observed at 150°W (see Figure 8 in section 2*b*), but the depths of the layers of eastward and westward moving water at 170°E and 150°W differ considerably.

There are several sets of measurements to depths of about 200 meters that corroborate the complicated vertical structure just described. The measurements of *Masuzawa* [1967] at 0°, 137°E in the winter of 1967 and measurements at 3°N, 137°E in May 1933 and at 1°N, 155°E in January 1928 that *Tsuchiya* [1961] brought to attention show eastward surface flow, a westward drift below that, and a deeper eastward current. This was also the profile at 140°E between February 6 and 8, 1964, when the maximum of the subsurface westward flow was at 75 meters [*Istoshina and Kalashnikov*, 1965]. *Yosida et al.* [1959] documented a similar situation at 153°E between January 23 and 29, 1958, and at 0°, 151°E between January 29 and February 3, 1958. It is noteworthy that all these observations were made during the winter months, when the winds usually have an eastward component. A more accurate indication that the winds were indeed eastward is the eastward surface flow at the equator. In the future we shall, in the absence of wind data, use the direction of the surface flow at the equator as an indication of the direction in which the wind was blowing. Note, however, that the flow at the equator is frequently eastward during periods of calm weather.

The structure of the currents above the permanent eastward current in the thermocline changes quite dramatically when the wind direction changes from east to west. During the months March, June, July, and August of 1967, the winds at the equator at 170°E were from the east. Figure 3*b*, a representative example, shows the shear of the zonal flow superimposed on the temperature profile, as observed on March 26, 1967. Contrast this with figure 3*a*, which shows the current structure in April 1967, when the winds were from the west. Note that in March the current had two eastward cores, one in the homogeneous layer, the other in the thermocline, separated by a layer of maximum vertical temperature gradient. (This double-celled structure was first observed by *Noel and Merle* [1969].) The upper eastward cell, the one that was in the homogeneous layer and that was not in geostrophic balance, became a westward jet when the winds started blowing from the west. The lower of the two eastward cores, the one that was in the thermocline and that had its downstream flow in geostrophic balance [*Colin and Rotschi*, 1971] remained an eastward core. The change in wind direction affected the deep westward current even less than the eastward undercurrent.

There is further evidence of westward surface flow and subsurface eastward flow with a bicellular structure from measurements at 153°E and at 149°E in mid-February 1958 [*Yosida et al.*, 1959]. It was suggested in the introduction (section 1) that the conditions for an undercurrent with two cores may be stringent, so that it is not surprising that the eastward subsurface flow at 155°E in February 1958 [*Yosida et al.*, 1959] did not have two cells and that *Tsuchiya* [1961] does not report such a phenomenon. An alternative explanation for the absence of two eastward cells in these measurements could be that the vertical spacing of the velocity measurements was too large.

The impression gained from the observations described thus far is that of variable flow in the surface layers (eastward surface flow and westward subsurface flow, or vice-versa) and of permanent currents below the mixed layer (eastward flow in the thermocline and westward flow at greater depths). The latter two (deeper) currents may vary in intensity but seldom change direction. *Montgomery* [1962] assembled all available western Pacific stations within 70 miles of the equator and found that 95% of them indicated an eastward flow at 150 meters and 85% indicated an eastward current at 200 meters. However, there have been cases that do not conform to either of the two zonal velocity profiles described thus far. The other possibilities documented correspond to either eastward flow from the surface to below the thermocline (between February 2 and 8, 1958, at 147°E [*Yosida et al.*, 1959; *Tsuchiya*, 1961, Figures 43 and 30]) or westward flow from the surface to 800 meters [see *Tsuchiya*, 1961, Figures 48 and 43]. Tsuchiya, incidentally, mentions several possible sources of error in the measurements, especially depth measurements, on which he reports.

The southern edge of the North Equatorial Countercurrent fluctuates seasonally between 2°N and 4°30′N [*Yamanaka et al.*, 1965; *Burkov et al.*, 1960], so that it is frequently joined to the undercurrent by a continuous band of downward-sloping eastward-flowing water [see, e.g., *Yosida et al.*, 1959; *Burkov and Ovchinnikov*, 1960]. On such occasions the presence of a thermal front at the southern edge of the countercurrent makes a distinction between the undercurrent

and the countercurrent possible [*Burkov*, 1963, 1966; *Burkov et al.*, 1960; *Hisard et al.*, 1969]. Convergent flow is usually associated with the presence of a front. In March 1967 at 170°E, when the winds were easterlies, *Hisard et al.* [1970] observed convergences at 3°N and 3°S and a divergence close to the equator (at 0°30′N). At the bottom of the mixed layer (at the level of the upper core of the eastward undercurrent), equatorward flow was measured at 1°N and 1°S. Further clues to the nature of the meridional circulation near the equator are indirect.

The structure of the density field in a meridional plane is marked by a deep mixed surface layer at the equator and below that by a downward-spreading equatorial thermocline. The depth of the mixed layer at 170°E is approximately 150 meters. Farther west the mixed layer becomes shallower; it is less than 50 meters deep west of 137°E. (Whether a bicellular undercurrent is possible when the mixed layer is very shallow has yet to be determined.) Practically all the observations mentioned thus far show an equatorial spreading of the thermocline below the homogeneous layer. Lines of constant salinity and oxygen concentration also appear to trough at the level of the eastward flow in the thermocline. Relative to the neighboring water on the same isanosteric surface, the water of the eastward undercurrent in the thermocline (above 160 cl/t) is rich in oxygen and poor in phosphate. On isanosteric surfaces below 160 cl/t, the water in the deep westward-flowing Intermediate Equatorial Current (below 160 cl/t) is poor in oxygen and rich in phosphate [*Rotschi and Wauthy*, 1969]. The neighboring water at such depths apparently flows eastward and is rich (relative to the deep westward equatorial current) in oxygen [*Hisard and Rual*, 1970]. From the water properties one may infer either that there is downwelling in the equatorial thermocline above the 160 cl/t surface and upwelling below that, or that the source of the eastward-flowing water above the 160 cl/t surface is rich in oxygen, whereas the source of the westward-moving water below it is poor in oxygen, or that both possibilities have elements of truth.

*Hisard et al.* [1969], on comparing five sections made between March and August 1967 across the equator at 170°E, find that the undercurrent is most intense and has a maximum transport (as measured from the surface to 400 meters and from 4°S to the southern edge of the countercurrent) in July (55 Sv) and a minimum in April (15 Sv). If this is a seasonal variation, it is in phase with the variation of the North Equatorial Countercurrent. This very variable current, which has an average transport of 40 Sv and which decreases in intensity downstream, is most intense in late summer and weak from March to June [*Burkov et al.*, 1960; *Wyrtki and Kendall*, 1967; *Yamanaka et al.*, 1965]. The arithmetic mean of the combined undercurrent-countercurrent transport is thus 75 Sv. This is the value *Yosida et al.* [1959] assign to it at 150°E in January and February 1958. At the moment it is not possible to describe the deep westward currents quantitatively. On the basis of a meridional section along 137°E during the winter of 1967, *Masuzawa* [1967] estimates a net eastward flux of 36 Sv between 2°N and 33°30′N. This included the North Equatorial Current. At that time strong eastward flow was also measured at 1°N and at the equator. From arguments involving the conservation of mass, *Masuzawa* [1967] concludes that the neglected deep westward currents must be important.

*b. The central Pacific: The Gilbert Islands (174°E) to the Galapagos Islands (92°W).* In the introduction it was suggested that if the vertical stability at the base of the homogeneous layer is large, two independent subsurface eastward currents separated by the layer of strong stability are possible in the presence of a westward wind. An eastward wind, on the other hand, could lead to eastward surface flow and, at the base of the homogeneous layer, to westward subsurface flow. Such profiles have been observed in the western Pacific and should also be possible in the western part of the central Pacific, since a homogeneous surface layer is present as far east as 140°W (see Figure 7). *Istoshina and Kalashnikov* [1965] observed the latter of the two profiles just described at the 180° meridian in December 1962 and January 1963. Their shear measurements indicated eastward flow with a maximum at the surface, a zero at about 100 meters, and a second maximum in the thermocline at 200 meters. The other possibility, westward surface flow driven by westward winds and, below that, eastward flow with a bicellular structure, occurred west but not east of 150°W in February 1969 [*Colin et al.*, 1971]. As was mentioned earlier, special conditions are necessary for a bicellular structure to be possible, so that it is not surprising that the undercurrent had one core only at 156°W in February 1970 [*Colin et al.*, 1971], at 154°W in the autumn of 1961 [*Koshlyakov and Neyman*, 1965], and at 150°W in the spring of 1971, when in the face of the southeast trades the eastward flow extended from the surface to a depth of 500 meters and attained speeds up to 162 cm/sec [*Taft et al.*, 1973]. East of 140°W, where there is no deep homogeneous surface layer (see Figure 7) and where the winds do not reverse direction seasonally, the permanent, subsurface eastward undercurrent has never been observed to have more than a single cell in the vicinity of the thermocline.

The presence of the deep westward Intermediate Equatorial Current below the undercurrent has been established by *Istoshin and Kuklin* [1962] at 1°N, 154°W, by *Knauss* [1960, 1966] at several locations east of 140°W, and by *Taft et al.* [1973] at 150°W, where the layer of westward flow extended from 470 meters to a depth greater than 1000 meters, with a maximum speed of 38 cm/ sec at a depth of 750 meters at 1°S (see Figure 8); the maximum westward velocity at the equator was 27 cm/sec.

*Knauss* [1962] inferred eastward flow near the ocean bottom at the equator from an analysis of deep temperature measurements. A flow with such a component has been measured by *Taft et al.* [1973] over a period of four and a half months at a depth of 3500 meters at 150°W and by *Taft and Jones* [1973] 15 meters off the bottom at 115°W. At 115°W the shear between 15 meters and 500 meters above the bottom was found to be relatively large ($2 \times 10^{-5}$ sec$^{-1}$), a possible indication that a benthic boundary layer was present, or a consequence of the local bottom topography.

The eastward flow observed by *Taft et al.* [1973] at 150°W had a deep (360 meter) secondary maximum (25 cm/sec) well below the thermocline (see Figure 8). A similar feature has been observed by Taft and Jones at 0°, 115°30′W, by *Taft and Knauss* [1967, section 7] in the Indian Ocean, and by *Voigt et al.* [1969] in the eastern Atlantic. It is possible that this secondary maximum is an intermittent phenomenon; it is absent from *Knauss*'s [1966] measurements at

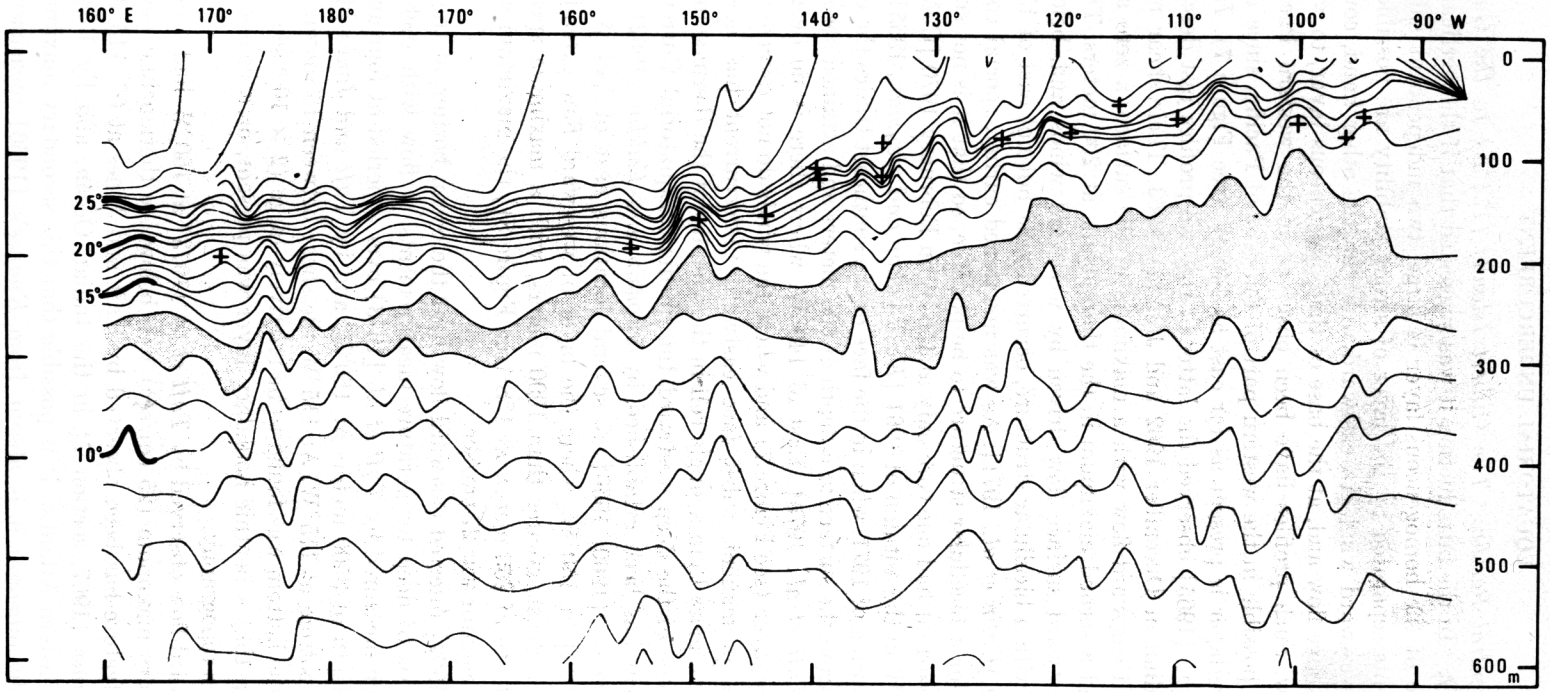


Fig. 7. Isotherms in an equatorial plane in the Pacific. [After *Colin et al.*, 1971.]

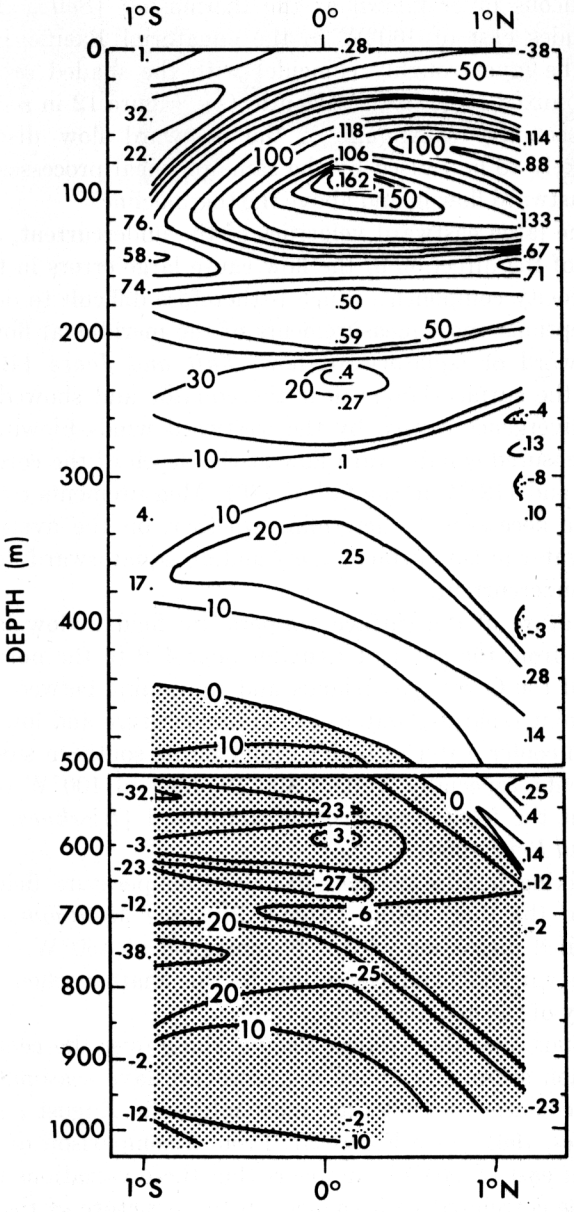


Fig. 8. Vertical structure of the zonal flow (centimeters per second) in a meridional plane at 150°W in the spring of 1971. The numbers give the values of the extremums in the vertical profile. The shaded area indicates westward flow. [After *Taft et al.*, 1973.]

0°, 118°W. (Its absence could also be due to measurement error.) It is intriguing that *Taft and Jones* [1973] found the secondary maximum to be located at the base of a layer of low vertical stability. This mixed layer is apparently part of

the deep homogeneous layer known as the thermostad [*Seitz,* 1967], which is present at longitudes east of 160°W in the equatorial Pacific [*Stroup,* 1969]. The position of the layer roughly coincides with the shaded area in Figure 7. There is a similar mixed layer in the Atlantic (see Figure 12 in section 2*d*). Note that the deep secondary maximum of the eastward flow discussed in this paragraph is unlikely to be caused by the same physical processes that give rise to the bicellular eastward flow in and above the thermocline.

Because of the large eastward velocities of the undercurrent, small errors in the measurement of the direction of the flow cause large errors in the estimate of the meridional velocity component, which is therefore difficult to determine. With the following exceptions, most measurements of the meridional flow do not show a consistent poleward or equatorward flow. *Taft and Jones* [1973] measured poleward flow in the surface layers near the equator and showed it to be consistent with the divergence caused by the westward winds blowing at the time. *Knauss* [1966] measured equatorward flow at the depth of the core of the undercurrent at 140°W and 118°W in the fall of 1961. Measurements over an extended period of time are necessary to determine whether, on the average, there is a poleward flux of water in the surface layers and an equatorward flow at the level of the core of the undercurrent.

A peculiar feature of the surface temperature field in low latitudes is the front that extends from the coast of Ecuador near 4°S to the northwest, cutting the equator east of the Galapagos Islands and continuing between 1°N and 3°N to the west. The front separates water of high temperature and low salinity on its northern side from cooler water of high salinity on its southern side. It is subject to lateral movements, especially west of 100°W. East of 100°W opposing winds apparently prevent the front from drifting southward [*Bjerknes,* 1961; *Wyrtki,* 1966; *Cromwell and Reid,* 1956].

The most striking feature of the subsurface temperature field is the equatorial spreading of the thermocline (Figure 2). (See *Montgomery and Stroup* [1962] for a detailed discussion of this phenomenon at 150°W.) The degree of spreading is quite variable, and we return to this matter when discussing the seasonal variability of the undercurrent.

Unlike the winds over the western Pacific, those over the central Pacific do not reverse direction seasonally. They do, however, have seasonal variations in their intensity: the southeast trades are most intense in August and are weakest in March [*Bjerknes,* 1961] (see Figure 5). From a comparison of measurements of the undercurrent east of 140°W it appears that these variations in the strength of the wind may be correlated with changes in the structure of the undercurrent. The most detailed measurements east of 140°W are those made on the *Dolphin* cruise in April and May 1958 [*Knauss,* 1960] (on that cruise a meridional section was made at 140°W only); the *Swansong* cruise between September and November 1961 [*Knauss,* 1966]; the *Eastropac* cruise, which occupied an equatorial station on April 1, 1968 [*Jones,* 1969]; and the *Piquero* expedition from June 26 to August 4, 1969 [*Taft and Jones,* 1973]. (For a detailed comparison of the four sets of data the reader is referred to *Taft and Jones* [1973].) Four sets of data are obviously not sufficient for the purpose of establishing a correlation. It is of course

possible to describe hypothetical, systematic variations that are consistent with the available evidence. Later we furnish supporting evidence for such trends from observations in other ocean basins. Note that the changes in the structure of the undercurrent to be discussed are much larger than either the observed daily and weekly variations to which it is subject or the possible errors in measurement.

The strength of the westward South Equatorial Current at the surface seems to be proportional to the intensity of the southeast trades. From *Wyrtki*'s [1965] monthly charts of the surface circulation of the eastern, tropical Pacific Ocean it is apparent that this current is most intense between July and November and weakest in March, April, and May. The four sets of measurements referred to in the previous paragraph conform to this pattern. *Knauss* [1966] measured a westward surface velocity of 95 cm/sec at 1°N, 96°W in the autumn of 1961. *Jones* [1969] in April 1968 and *Taft et al.* [1973] in the spring of 1971 (on an occasion when the winds were westward) observed eastward surface flow at the equator. Such a current is common in both the eastern part of the Pacific and the Atlantic in April and May; it is referred to as a surfacing of the undercurrent and was first noted by *Puls* [1895].

Figure 9 shows the zonal velocity profile observed on three different occasions, under different wind conditions, near 97°W. (Velocity measurements were not made at 97°W during the *Piquero* expedition, but those measurements that

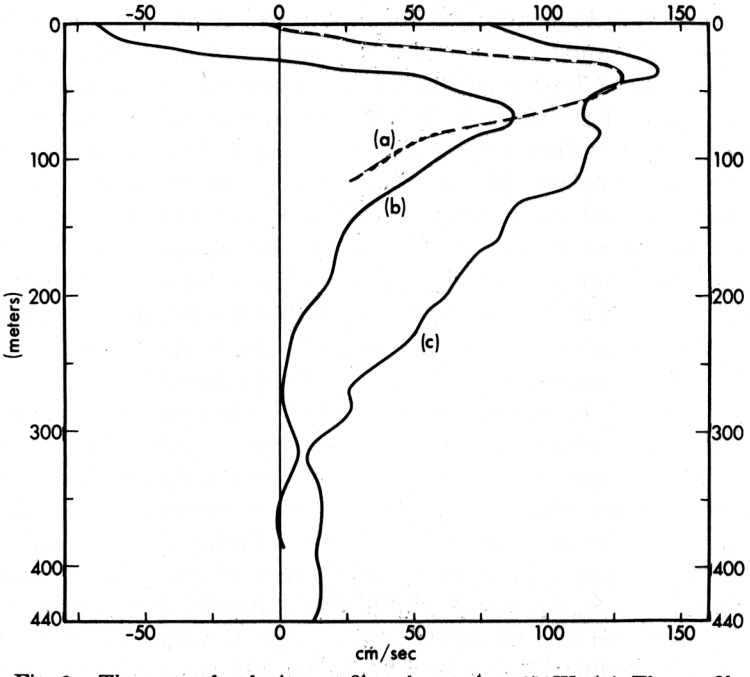


Fig. 9. Three zonal velocity profiles observed at 97°W. (*a*) The profile in May 1958, when the winds attained speeds of 3.3 m/sec. (*b*) The profile in October 1961, when the winds attained speeds of 8 m/sec. (*c*) The profile in April 1968, when the winds attained speeds of 1.5 m/sec. [After *Knauss*, 1960, 1966; *Jones*, 1969.]

were made between the Galapagos and 115°W on that expedition are very similar to the measurements made in October 1961, when the wind conditions were similar.) It is consistent with the measurements in Figure 9 to say that the more intense the westward winds are, the stronger is the westward surface flow and the weaker and shallower is the core of the undercurrent. Comparison of the measurements of *Knauss* [1960, 1966] and *Colin et al.* [1971] at 140°W supports this conjecture. *Brosin and Nehring* [1968] observed a similar relation between the wind and current speed at 30°W in the Atlantic (see section 2*d*). The eastward transport of the undercurrent is similarly affected by changes in wind conditions. Its value at 140°W in October 1961 was one half of what it had been (39 Sv) at the same longitude in May 1958. The transports at 118°W and 15.5°W, measured at different times but under similar wind conditions on the *Swansong* and *Piquero* expeditions, respectively, were nearly the same (20 and 19 Sv, respectively).

*Knauss* [1960] found the undercurrent to have a high degree of symmetry about the equator at 140°W in the spring of 1958 but to be less symmetric at the same longitude in the fall of 1961. A possible explanation is that the northward component of the wind, stronger in the fall than in the spring, causes a meridional pressure gradient that forces an upwind shift of the core of the undercurrent. Consistent with this view is the more pronounced asymmetry of the undercurrent further to the east, where the winds have a stronger northward component [*Bjerknes*, 1961] (see Figure 5). (The meridional sections of the zonal flow east of 140°W all show an undercurrent that is better developed south than north of the equator, but only *Christensen*'s [1971] measurements reveal an undercurrent with its core south of the equator. Perhaps the latitudinal spacing (1°) of the measurements on the other cruises was too large.) The possibility that the proximity of the Galapagos Islands affects the symmetry of the undercurrent cannot be ruled out; all the meridional sections east of 140°W were made under similar wind conditions in the autumn. Neither the closeness of the Galapagos Islands nor a wind-induced southward pressure force explains why *Colin et al.* [1971] found the core of the undercurrent south of the equator at 154°W on an occasion when the winds were from the east northeast. Could the horizontal shear of the wind and the proximity of the ITCZ have been a factor?

In the spring of 1958 when *Knauss* [1960] observed the thermocline to spread symmetrically about the equator, a well-mixed surface layer was absent at the equator (see Figure 2). There was at the time a deep penetration of water of high oxygen and low phosphate and silicate concentration, as is evident from Figure 10. Note that the upper isopleths in Figure 10 ridge. The cold surface water therefore had a low oxygen and high phosphate content. Such characteristics suggest upwelling [see, e.g., *Cromwell*, 1953]. The unusually high temperature and high oxygen values and low phosphate and low silicate values below the thermocline suggest downwelling [*Philander*, 1973]. In addition, strong vertical mixing probably contributes to the anomalous distribution of properties at the equator [*Knauss*, 1966].

As with the velocity field, the above hydrographic features are considerably modified when the winds gain in intensity. The meridional section at 140°W made

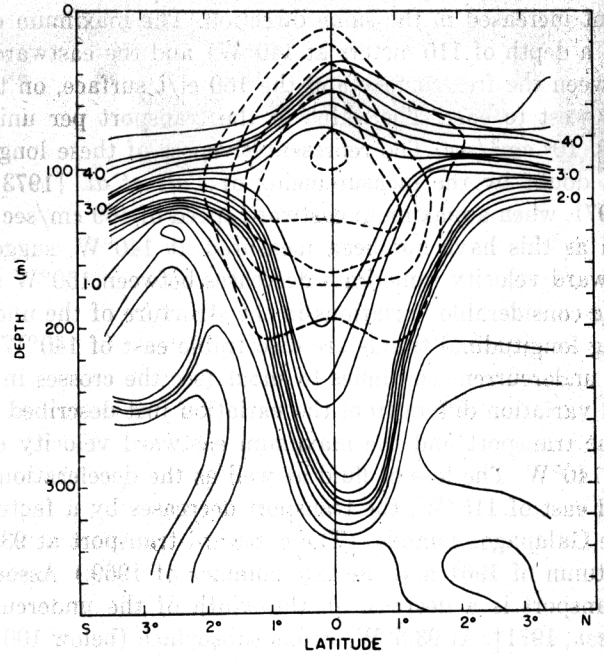


Fig. 10. An oxygen cross section (in milliliters per liter) superimposed on a velocity cross section at 140°W in May 1958. The interval of the velocity contours (in dotted lines) is 25 cm/sec. The maximum velocity is 125 cm/sec. [After *Knauss*, 1960.]

on the *Swansong* cruise shows hardly any troughing of the isopycnals (see Figure 2). Not only is there little evidence of troughing isotherms from the section at 118°W, but the isotherms at that longitude at that time were also asymmetric about the equator [*Knauss*, 1966]. The meridional sections made on the *Piquero* expedition are similar to those just described.

Whereas an undercurrent that is symmetric about the equator can have its downstream flow in geostrophic balance, an asymmetric undercurrent has not been observed to have the Coriolis acceleration of the zonal component of its flow in balance with the meridional component of the pressure force. From an inspection of the meridional momentum equation one expects ageostrophic conditions when the flow across the equator at the core of the undercurrent becomes large. It is yet to be determined how large this meridional flow has to be. It is also unclear whether it is possible for the downstream flow (as opposed to the zonal component) of the undercurrent to be in geostrophic balance when the downstream direction is at an angle to the equator.

Meridional sections at 140°W, 148°W, and 156°W by *Colin et al.* [1971] between January 15 and February 11, 1970, when the winds were from the ENE with a speed of 8 m/sec, enable us to describe the longitudinal variations of the current in that region at that time. The westward surface flow had a mean speed of 50 m/sec and increased slowly from east to west. The depth of the core of

the undercurrent increased in the same direction. The maximum eastward speed (100 cm/sec at a depth of 110 meters at 140°W) and the eastward transport per unit width between the free surface and the 160 cl/t surface, on the other hand, increased from west to east. The value of the transport per unit width at 0°, 140°W was $9 \times 10^5$ cm$^2$/sec. The representativeness of these longitudinal variations is put in doubt by the measurements of *Taft et al.* [1973] at 150°W in the spring of 1971, when a maximum eastward speed of 169 cm/sec was measured. Speeds as high as this have not been measured at 140°W, suggesting that the maximum eastward velocity sometimes decreases between 150°W and 140°W.

Despite the considerable variations in the structure of the undercurrent, certain unchanging longitudinal trends are discernible east of 140°W. In this region the core of the undercurrent continues to shoal (see the crosses in Figure 7), but its longitudinal variation differs from the variation just described west of 140°W in that both the transport and the maximum eastward velocity decrease downstream east of 140°W. The loss of fluid as well as the deceleration of the current is most marked east of 115°W; the transport decreases by a factor of 2 between 115°W and the Galapagos Islands. (The eastward transport at 93.5°W was 8 Sv in both the autumn of 1961 and the late summer of 1969.) Associated with the diminishing transport is a decrease in the width of the undercurrent [*Knauss*, 1966; *Christensen*, 1971]. At 93.5°W, strong subsurface (below 100 meters) northward flow was measured at the equator and north of the equator during both the *Piquero* and *Swansong* cruises. This suggests that the undercurrent flows along the northern side of the Galapagos Islands. It has not been established whether the decrease in transport of the undercurrent is due to upwelling and poleward drift in the South Equatorial Current or to downwelling into the deep Intermediate Equatorial Current. Analysis of the oxygen content of the water in the core of the undercurrent and of the neighboring water at the same depth gives no evidence of a poleward loss directly from the core of the undercurrent [*Taft and Jones*, 1973].

The eastward transport of the undercurrent, we have noted, is at a maximum in the spring and at a minimum in the fall. If so, it is out of phase with the South Equatorial Current and the Equatorial Countercurrent. Both these currents are weak in April and May and intense during the late summer. *Wyrtki* [1966] has attempted a quantitative description of the circulation in the eastern Pacific for the period from June to December, but it will have to be revised because he takes the transport of the undercurrent to be 35 Sv (it probably does not exceed 22 Sv in the autumn) and neglects the (unknown) transport of the Intermediate Equatorial Current.

When the undercurrent is symmetric about the equator, it is possible for the downstream flow to be in geostrophic balance. This is not true of the meridional flow. Measurements show that in the zonal momentum balance both the nonlinear advection of momentum and the longitudinal pressure gradient are important. This pressure gradient is a consequence of the slope of the isotherms (see Figure 7). *LeMasson and Piton* [1968] have compared the various computations (which use different sets of data, and different reference levels) of isobaric surfaces in the Pacific. It appears that the sea surface slopes down toward the east along the

equator with an inclination of about $5 \times 10^{-8}$. This slope corresponds to an eastward pressure gradient of $5 \times 10^{-5}$ dyne/g at the surface. At the depth of the core of the undercurrent it is smaller by a factor of more than 2. The slope of the sea surface is not uniform: according to *Knauss* [1963] it has a maximum ($6.5 \times 10^{-8}$) between 120°W and 170°W; the sign of the slope of the sea surface appears to reverse in the vicinity of the Gilbert Islands [*Austin*, 1958; *LeMasson and Piton*, 1968). *Knauss* [1966] asserts that there is a reversal in the sign of the zonal pressure force at the sea surface at 98°W and at the depth of the undercurrent at 104°W, but *Taft and Jones* [1973] do not find the evidence convincing —apparently the slope is too small for a clear trend to be discernible. The eastward pressure force between 140°W and 156°W as calculated by *Colin et al.* [1971] differs from the pressure force calculated by the other authors just mentioned in an important respect. Colin et al. find that it becomes westward just below the core of the undercurrent (at 150 meters). This is presumably the source of momentum for the deep westward equatorial current. All the calculations of isobaric surfaces are relative to some arbitrary surface. Pressure gages on the ocean floor together with density measurements above are necessary for accurate measurements of the zonal pressure gradient that presumably drives the equatorial currents.

*c. The Galapagos Islands to Ecuador.* Velocity measurements just west of the Galapagos Islands indicate flow with a strong northward component. This, together with measurements at 1°N, 0°, and 1°S along 87°W (to the east of the Galapagos) that showed subsurface eastward flow with a maximum (25 cm/sec) north of the equator, led *Knauss* [1966] to postulate that the undercurrent flows around the northern rather than southern side of the Galapagos Islands. *Knauss* [1966] also suggested that there may be no loss of transport as the undercurrent flows around the islands. This appears to have been the case at the time of *Christensen's* [1971] measurements. Christensen estimates the transport at both 92°W (west of the Galapagos) and 89°W (east of the Galapagos) to be 3 Sv. *Knauss's* [1966] value for the transport at 87°W is 4 Sv. From the measurements of *Knauss* [1966] and *Christensen* [1971] it would appear that the effect of the Galapagos Islands on the undercurrent as it flows around the islands is to weaken the downstream velocities, to deepen the depth of the core, and to spread the undercurrent over a larger meridional distance.

*Stevenson and Taft* [1971] have reviewed the analyses of temperature, salinity, and oxygen data for the equatorial region east of the Galapagos. They conclude that there is a close association between the undercurrent and a high-salinity core, the location of which frequently coincides with the southern edge of the earlier-mentioned equatorial front. This claim is substantiated by the measurement of eastward velocities of up to 37 cm/sec (relative to the flow at a depth of 310 meters) in the high-salinity core at 84°W in June 1969. The salinity core can be traced eastward across the Pacific (it is usually south of the equator) to the Galapagos [*Knauss*, 1966; *Tsuchiya*, 1968]; it is probably deflected southward around the islands. This would imply that the undercurrent has a southern branch [*White*, 1969]. If the high-salinity core is indeed a tracer of the undercurrent, the undercurrent veers in a southeastward direction at 82°W and is present

to within 110 km of the coast of Ecuador and northern Peru [*Stevenson and Taft*, 1971].

*d. The Atlantic Ocean.* Before 1963 it was thought that the current that flows in a northwestward direction from Cap São Roque (about 5°S) along the coast of Brazil transports water from the southern hemisphere to the Caribbean Sea. Measurements taken off northeastern Brazil since 1963 have caused a revision of ideas about the circulation pattern in that area [*Cochrane* 1963, 1965, 1966; *Williams*, 1966; *Metcalf and Stalcup*, 1967; *Metcalf*, 1968; *Ingham and Elder*, 1970]. It now appears that the coastal current has a discontinuity in the vicinity of the mouth of the Amazon River. In that region its southern part, referred to as the North Brazilian Coastal Current by *Metcalf and Stalcup* [1967], curves back on itself (see Figure 11) and becomes the Equatorial Undercurrent. The continuation of the northwestward coastal current, the part north and west of the Amazon, known as the Guiana Current, is sustained by the westward North Equatorial Current, which is located north of 9°N in mid-ocean. The North Equatorial Current and the North Brazilian Coastal Current jointly sustain a third current, the eastward North Equatorial Countercurrent. This current, which resembles the undercurrent in being much richer in oxygen and salt than the currents adjacent to it, can be found between 5°N and 9°N (north of the

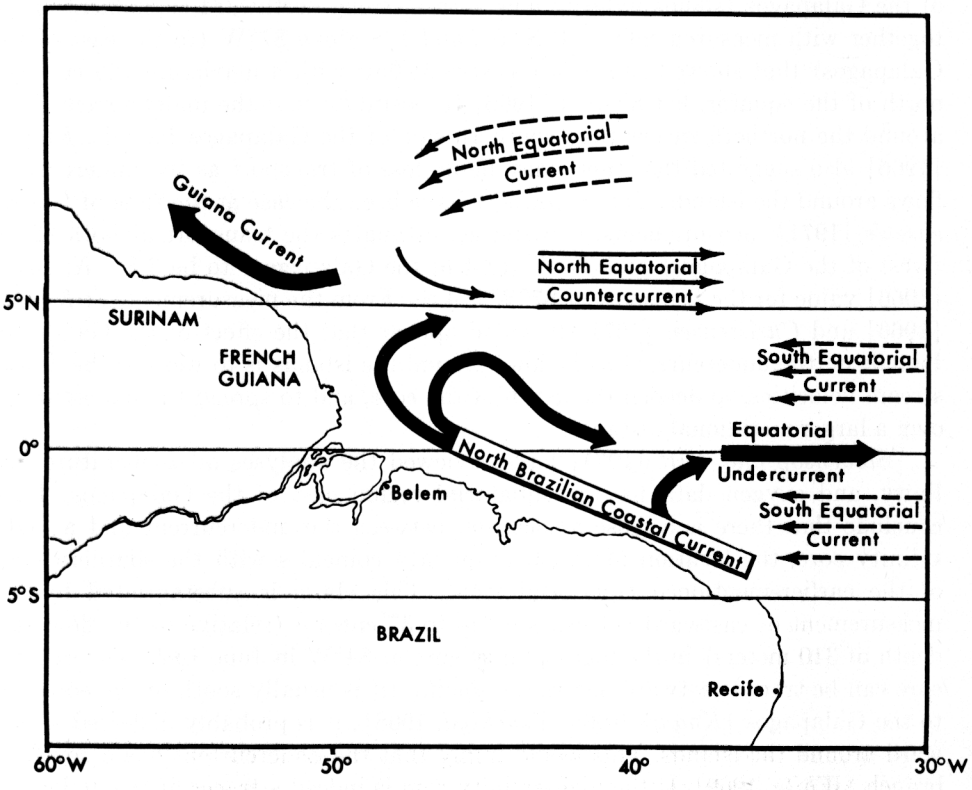


Fig. 11. A schematic drawing of the circulation in the western equatorial Atlantic.

westward South Equatorial Current). It is continuous across the Atlantic from August to November, when it feeds the eastward Guinea Coastal Current. During the rest of the year it frequently disappears from the surface of the western Atlantic [*Defant,* 1961; *Knauss,* 1963; G. Neumann, private communication, 1973]; on such occasions it may be present as a subsurface current [*Metcalf and Stalcup,* 1967].

The above description is a simplified version of what happens in the vicinity of the mouth of the Amazon. In reality, the North Brazilian Coastal Current goes through various time-dependent convolutions and meanders before becoming the Equatorial Undercurrent. Even as far east as 33°W, *Ingham and Elder* [1970] found the structure of the undercurrent to be quite variable over a period of days. From about 30°W to within 80 nautical miles (150 km) of the African coast, the Equatorial Undercurrent is a permanent feature of the equatorial circulation. Its most outstanding feature is a subsurface core of water of very high salinity (usually in excess of 36.2‰; see Figure 12). The undercurrent derives this core from the North Brazilian Coastal Current; there is no evidence of advection of high-salinity water into the undercurrent east of 35°W. In the spring of 1965 at 8°W the high-salinity core, as defined by the 35.8‰ isohaline, was approximately 200 km wide and 60 meters thick. Vertical gradients of salinity in the core were as high as 0.2‰ within 3–6 meters. The center of the core was at a depth of about 60 meters [*Rinkel,* 1969]. Note, however, that the core oscillates in both a vertical and a horizontal plane (see section 5). Though the region of maximum salinity is closely associated with the region of highest eastward velocity, the two maximums need not coincide: *Voigt et al.* [1969] found the maximum current to be

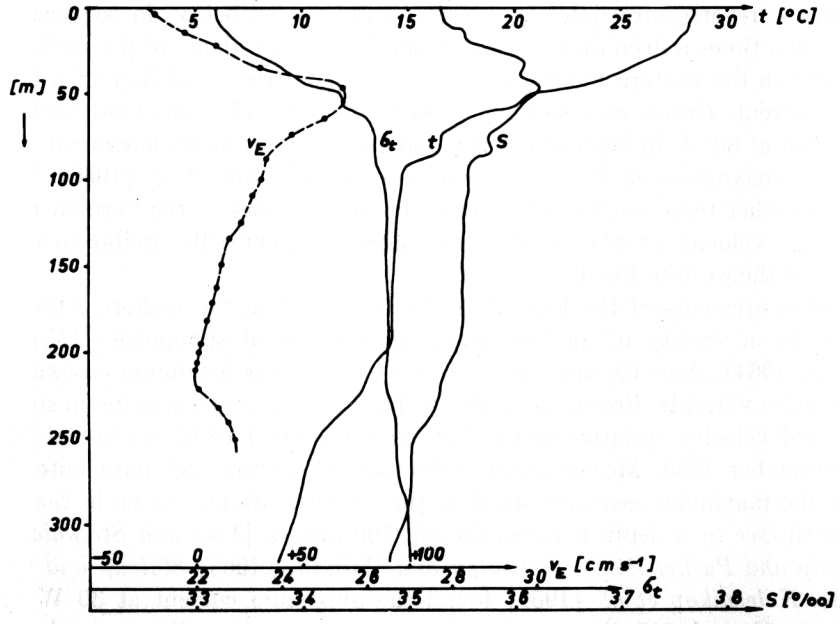


Fig. 12. The temperature, salinity, $\sigma_t$, and current shear at 0°07'N, 11°56'W in April 1964. [After *Voigt et al.,* 1969.]

below the salinity maximum; *Rinkel* [1969] found it to be above the salinity maximum.

Except for the subsurface core of water of extremely high salinity, the Equatorial Undercurrent in the western part of the Atlantic, where the southeast trades prevail, is very similar to its counterpart in the central Pacific. The undercurrent is usually sandwiched between westward flow at depth and westward surface flow except when the winds die out for a period of time, on which occasions the undercurrent surfaces [*Puls,* 1895; *Voigt,* 1961]. A deep westward current attaining speeds in excess of 30 cm/sec has been measured over a period of two months at 0°, 35°W at a depth of 405 meters by *Stalcup and Metcalf* [1966]. The measurements of *Ponomarenko* [1962] show the equatorial flow to have a westward component at depths of 1000 meters and 1200 meters (but not at 800 meters).

The Equatorial Undercurrent in the Atlantic, as elsewhere, is characterized by an equatorial spreading of isotherms and oxygen isopleths [*Metcalf et al.,* 1962; *Reid,* 1964; *Neumann and Williams,* 1965). Figure 12 shows vertical profiles of temperature, density, salinity, and zonal velocity near 0°, 12°W in April 1964. A layer of low vertical stability similar to the one in the Pacific is clearly discernible below the core of the undercurrent [see also *Rinkel,* 1969]. The eastward velocity is seen to have a secondary maximum just below the thermostad. (Taft and Jones found the secondary maximum at the base of the thermostad in the Pacific.)

The depth of the mixed surface layer at the equator in the Atlantic is variable. Because of the equatorial spreading of the thermocline there is at times no mixed layer [*Metcalf et al.,* 1962]; on other occasions it can have a depth of about 50 meters [*Brosin and Nehring,* 1968]. The winds over the Atlantic are not known to reverse direction periodically, but they probably do so occasionally. If at such times a deep mixed layer should be present, then, on the basis of what happens in the western Pacific, one cannot rule out the possibility of a bicellular undercurrent. *Brosin and Nehring* [1968] claim to have observed such a phenomenon at 30°W in September 1966 and find hints of an undercurrent with two or more maximums in the measurements of *Kolesnikov et al.* [1966]. It is unclear whether these maximums are merely irregularities in the vertical profile of the zonal velocity or whether they are indeed distinct cells similar to those observed in the western Pacific.

Measurements of the Equatorial Undercurrent in the western Atlantic, obtained by a variety of methods including the use of submarines [*Crease and Pogson,* 1964], show its structure and, in particular, its maximum eastward speed to be quite variable. *Brosin and Nehring* [1968] measured a maximum subsurface eastward velocity (relative to the flow at 300 meters) of 57 cm/sec at 29°30′W in September 1966. Measurements with current meters and parachute drogues show the maximum eastward speed in the western Atlantic to be in the vicinity of 80 cm/sec at a depth between 60 and 100 meters [*Voit and Strekalov,* 1964; *Stalcup and Parker,* 1965; *Neumann and Williams,* 1965; *Stalcup and Metcalf,* 1966]. *Kolesnikov et al.* [1966] found the maximum current at 30°W to vary between 80 and 107 cm/sec, depending on the season. *Ponomarenko* [1963] measured a maximum eastward speed of 116 cm/sec. According to *Metcalf et al.*

[1962] the undercurrent can attain a speed of 130 cm/sec, and the depth of the layer of eastward flow can be as much as 350 meters, but *Stalcup and Metcalf* [1966] caution that these values may be too high because they are based on shear measurements. Estimates of the transport of the undercurrent also vary considerably. Those who report a typical maximum eastward speed of 80 cm/sec estimate its transport to be approximately 14 Sv. However, the largest quoted value for the transport, 37.4 Sv at 18°W [*Khanaychenko et al.*, 1965], is considerably higher. If it is assumed that all these measurements are accurate, the variations must be related to changes in the wind conditions. Regrettably, not all the papers in which the measurements are presented give wind data; some of the papers give neither wind data nor the month in which the observations were made.

There are fortunately two sets of measurements, made by *Brosin and Nehring* [1968] at 29°30′W, that give indications as to how the structure of the undercurrent is affected by a change in wind conditions. In September 1966 when the southeast trades averaged 5 m/sec, the South Equatorial Current was intense (63 cm/sec at 0°30′N), and the maximum subsurface eastward velocity was 57 cm/sec at 0°30′S at a depth of 90 meters. The core of the undercurrent was south of the equator. (All measurements were relative to the flow at 300 meters.) In December 1966, when the winds at the equator were light or absent, the surface flow was eastward; the maximum subsurface eastward velocity, which was observed at the equator at a depth of 90 meters, had increased to 79 cm/sec (relative to 300 meters), and the undercurrent was better developed north than south of the equator. (At that time the ITCZ was at 2°N.) The surface waters near the equator were saltier and warmer in December than in September 1966. This is probably due to stronger eastward advection of warm, salty water in December than stronger equatorial upwelling in September. (Stronger upwelling would explain the lower sea surface temperature but, in view of the subsurface salinity core, would not explain the lower sea surface salinity in September.)

The southeast trades over the western part of the tropical Atlantic are usually weak in the spring and at their most intense in the autumn. It is therefore not surprising that the meridional sections of temperature and oxygen of *von Schemainda et al.* [1964] at 4°W in May 1964 show practically no evidence of equatorial upwelling. Isotherms, and especially isopleths of oxygen concentration do, however, trough in a pronounced manner at the equator. Also, *Rinkel* [1969] comments on the absence of isothermal doming near the equator at 8°W in the spring of 1965. The seasonal variations in the strength of the wind may also be the cause of the following observed variations in the structure of the undercurrent. Parachute drogue measurements at 8°W and 4°W show that the undercurrent was much more intense in the spring of 1964 (approximately 73 cm/sec at 8°W; *Rinkel et al.* [1966]) than in the autumn of 1964 (44 cm/sec at 8°W; *Gerard et al.* [1965]). A comparison of maps of salinity in the layer of maximum salinity in the equatorial Atlantic in the spring [*Williams*, 1966] and autumn [*Neumann*, 1969] of 1963 reveals that in the spring salinities in excess of 36.2‰ were found as far east as 2°E on the equator, but in the autumn the same isohaline closed off near 25°W. The low salinities measured by *Reid* [1964] at 10°W in July 1963, as compared with those measured by *Metcalf et al.* [1962] a mere

278 km further to the west in April 1961, testify to the considerable changes that are possible in the salinity field. These changes are consistent with a hypothetical weakening of the undercurrent from the spring to the fall. It is evident from a comparison of the above mentioned maps of salinity that the highest salinities were approximately on the equator in the spring of 1963 but were south of the equator in the fall of 1963. *Kolesnikov et al.* [1966] have observed a southward displacement of the core of the undercurrent between the spring and the fall.

The discussion thus far has concerned the undercurrent in the western Atlantic. The variations described will, of course, affect the undercurrent in the eastern part of the Atlantic. To complicate matters, the winds over the eastern tropical Atlantic (eastward of 10°W in August) are unlike those over the western tropical Atlantic in that the winds at the equator and north of it usually have an eastward component (see Figure 5).

One expects the eastward winds over the eastern Atlantic to cause a reversal of the sign of the zonal slope of the sea surface. Using data from a section along the equator completed in November 1958 by the R.V. *Crawford* [*Fuglister*, 1960], *Rinkel et al.* [1966] found that the sea surface at that time sloped down from west to east between South America and about 7°W, but that farther east it sloped upward. According to Rinkel et al.'s own measurements, the point at which the slope of the sea surface reversed was farther to the east (between 5° and 6°E near the island of São Tomé) in the spring of 1964.

The reversal of the slope of the sea surface implies a westward pressure force along the equator in the eastern Atlantic. One expects it to retard the undercurrent. The maximum eastward speed of the undercurrent did indeed decrease (nonuniformly but monotonically) from 80 cm/sec at 12°W to 30 cm/sec at 0°W in May and June 1964 (see *Sturm and Voigt* [1966] for measurements relative to 210 meters), and from a value in excess of 80 cm/sec at 4°E to 70 cm/sec at 6°E in March 1969 (see *Kolesnikov et al.* [1971] for measurements with current meters on unattended moorings). However, the current drogue measurements of *Rinkel et al.* [1966] in the spring of 1964, between 15°W and the coast of Africa, at the depth of the high-salinity core (not necessarily the same as the core of the undercurrent), show such large variations that no longitudinal trend is discernible. It is not possible to describe the longitudinal variation of the transport quantitatively, but it is noteworthy that everybody agrees that the transport of the undercurrent is lower in the eastern than in the western Atlantic. According to *Kolesnikov et al.* [1971] the difference can amount to a factor of 2.

Because the winds have a northward component and because of the proximity of the west African coast, the meridional pressure gradient in the eastern Atlantic is unlikely to be symmetric about the equator. Measurements by *Gerard et al.* [1965] show that the core of the undercurrent was south of the equator at 8°W and 4°W in September 1964. *Sturm and Voigt* [1966] observed a symmetric undercurrent at 4°W but found its core to be displaced increasingly to the south at 0° and 4°30′E in May and June 1964. According to *Kolesnikov et al.* [1971], isotachs of eastward flow extend farther south than north of the equator at both 4°E and 6°E. *Rinkel et al.* [1966] found that in the spring of 1964 the high-salinity core, which is closely associated with the undercurrent in the Atlantic,

disappeared from a zonal section along the equator near 6°E, after which it veered in a southeastward direction, terminating near 7°E, 1°30′S. A measurement at 8°E, 1°30′S (100 km from the African coast) indicated east-southeast flow of 38 cm/sec.

*Neumann's* [1969] chart showing the distribution of salinity at a depth of 50 meters in the Gulf of Guinea during the spring of 1964 shows the high-salinity water spreading toward the southeast in the termination area of the undercurrent. There is also an indication that another branch of high-salinity water spreads northeast from the equator. It is conceivable that this water joins the deep westward current measured below the eastward, surface Guinea Current by *Gerard et al.* [1965]. The details of the circulation in the Gulf of Guinea need clarification.

In conclusion we note that the undercurrent has been observed to split symmetrically about the equator on certain occasions (see Figure 13). *Neumann and Williams* [1965] at 15°30′W and *Koshlyakov and Neyman* [1965] at 176°W in the western Pacific have observed a similar phenomenon. It is noteworthy that the splitting occurs in regions where the undercurrent encounters a pressure force toward the west (G. Neumann, private communication, 1973).

*e. The Indian Ocean.* The most extensive observations at the equator in the Indian Ocean were made during the *Lusiad* expedition from June 28 to September 24, 1962, and from February 16 to May 15, 1963. Preliminary reports were published by *Knauss and Taft* [1963, 1964] and *Taft* [1967]; a detailed report appeared as a bulletin of the Scripps Institution of Oceanography [*Taft and Knauss,* 1967]. In this section, measurements made during the *Lusiad* expedition will be referred to by their date only.

The winds over the equatorial Indian Ocean are of the monsoonal type: between May and September, southwesterlies prevail; from November to March the winds are from the northeast; April and October are months of transition.

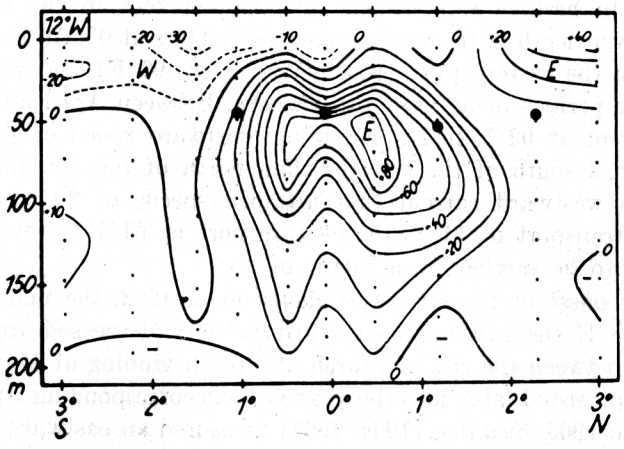


Fig. 13. Zonal velocity component in centimeters per second, relative to 215 meters, at 12°W in April 1964. [After *Sturm and Voigt,* 1966.]

In the Pacific and Atlantic the zonal pressure gradient in the tropic is set up by the southeast trades, which blow less dense water to the western side of the basin [*Montgomery and Palmén*, 1940; *Knauss*, 1963]. The vertical integral of the zonal pressure force then balances the westward component of the wind stress [*Arthur*, 1960]. In the Indian Ocean the zonal pressure gradient implied by the sloping isotherms depends on time, longitude, and depth in a complicated manner and is not as simply related to the surface winds. One nonetheless expects the northeast monsoon rather than the southwest monsoon to create conditions favorable for the presence of the undercurrent.

The sea surface temperature in the tropical Indian Ocean always increases from west to east, so that the upper isotherms slope downward from west to east. This implies a westward pressure force at the surface. The lower isotherms, however, were observed to slope upward to the east in March and April 1963. Thus, although the sea surface relative to 400 db sloped downward to the west in the spring of 1963, the lower isobaric surfaces sloped downward to the east. The reversal of the sign of the slope of the isobaric surfaces occurred at the 50-db level in the western part of the Indian Ocean and at the 75-db level in the eastern part. There was consequently an eastward pressure force at the depth of the equatorial thermocline, but not at shallower depths, in March and April 1963. After the onset of the southwest monsoon, the slope of the sea surface upward to the east increased, and by July 1963 it had reached a value of $5.2 \times 10^{-8}$. At that time isobaric surfaces down to 100 db all sloped upward to the east; the eastward pressure force at the depth of the thermocline had disappeared.

The northeast monsoon starts in November. In February 1961, *Ivanov* [1964] measured an eastward current of 63 cm/sec at a depth of 150 meters at 0°, 93°E. In 1963 the undercurrent formed much later; at 0°, 85°E the maximum eastward speed was 15 cm/sec in late February 1963 and 65 cm/sec in early April 1963. This suggests that not more than 45 days is necessary for the undercurrent to become established. The undercurrent in the spring of 1963 was at shallower depth in the western part (85 meters at 0°, 61°E) of the Indian Ocean than in the eastern part (110 meters at 0°, 92°E) and was observed to be stable over periods of at least three weeks. Between April 20 and 25, 1963, the undercurrent at 92°E had a maximum eastward speed of 81 cm/sec, was better developed south of the equator than north of the equator, was located above a deep westward current that attained speeds of 30 cm/sec, and had an eastward transport of 11 Sv. (The transport at 61°E a few weeks earlier was observed to be smaller by a factor of 2.)

After the onset of the southwest monsoon in 1963, the undercurrent grew weaker; at 53°E the maximum eastward velocity decreased from 34 cm/sec to 21 cm/sec between the end of March and the beginning of May. In 1964 the undercurrent persisted later into the year and, at corresponding times, was more intense than in 1963. *Swallow* [1964, 1967] measured an eastward flow of 100 ± 20 cm/sec at a depth of 75 meters at 0°, 58°E in March 1964. (Note that in 1967 Swallow revised downward the maximum eastward speeds that he had reported in 1964.) The winds at the time were light, but the mean easterly

winds were more intense in March 1964 than in March 1963. Taking the 50 cm/sec contour as the boundary of the undercurrent, Swallow estimates the eastward transport to have been 14 Sv. From the beginning of May onward, as the southwesterlies increased in intensity, the westward surface flow disappeared and the subsurface core of the eastward flow became weaker and asymmetric about the equator. The northward component of the winds appeared to cause an upwind (southward) displacement of the core of the undercurrent.

We noticed that the undercurrent weakened after the onset of the southwest monsoon in the early part of the summers of 1963 and 1964. Measurements at 53°E and 62°E in July and August 1962 and at 79°E on July 10, 1962, showed the undercurrent, as well as the features usually associated with it (the spreading thermocline, for example) to be absent. A pinching of the isotherms at the equator was in fact observed on a few occasions. Though there was no clear indication that the slope (upward from west to east) of isobaric surfaces reversed at depth, eastward flow was nonetheless observed in the thermocline at the equator at 79°E between August 31 and September 4, 1962 (see Figure 14). Note that the eastward surface flow and the westward core below it were both in the well-mixed layer. The situation is reminiscent of that in the western Pacific when the winds are eastward (see Figures 3 and 6). The flow at 89°E in September 1962 was similar to that observed at 79°E, but the undercurrent was

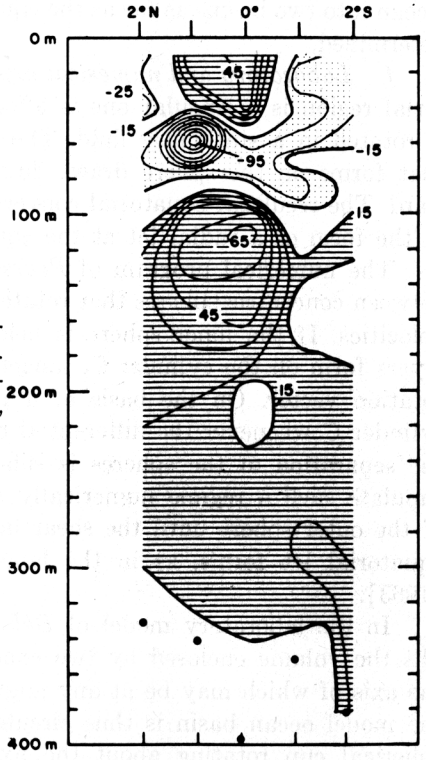


Fig. 14. The zonal velocity component (in centimeters per second) along 79°E in August 1962. East components are positive and westward components are negative. [After *Taft and Knauss*, 1967.]

more variable than it usually is in the spring; for example, between September 11 and 16 the maximum eastward velocity component at 89°E decreased from 51 to 34 cm/sec.

According to *Düing* [1969], the westward North Equatorial Current extends from the equator to between 5° and 8°N in the spring. At that time the North Equatorial Countercurrent is well developed and is present between the equator and about 5°S, whereas the South Equatorial Current is present as far south as 15°S. The South Equatorial Current is the most steady of the various currents in the tropical Indian Ocean. There is apparently no South Equatorial Countercurrent in the Indian Ocean. In the late summer, when there is eastward drift from 7°S to 15°N and from Africa to Sumatra, the North Equatorial Current disappears altogether. It is apparent that the undercurrent in the Indian Ocean is closely coupled to both the North Equatorial Countercurrent, from which it is not always distinguishable, and the Somali Current. Hence, when the high-salinity core in the equatorial thermocline at 58°E had a lower maximum salinity in June than in March 1964, *Swallow* [1967] attributed it to the Somali Current, which had reversed by June, causing less saline water to flow equatorward. We conclude that it is unlikely that measurements in the immediate vicinity of the equator only will be sufficient to determine the factors that affect the undercurrent in the Indian Ocean.

The Maldive Islands which cross the equator at 72°E leave only a very narrow channel for the undercurrent. Whether this effectively divides the Indian Ocean into two basins as far as the equatorial currents are concerned has yet to be determined.

*f. Laboratory and numerical experiments.* A demonstration that the equatorial region is a singular one is afforded by the experiment in which a sphere is rotated in a stationary fluid. The boundary layer (nonlinear Ekman layer) that forms on the sphere draws fluid from outside and transports it equatorward. The resultant equatorial convergence causes rupture of the boundary layer in the form of a radial jet at the equator [*Bowden and Lord*, 1963].

The numerical program of *Pearson* [1967] simulates the motion of a fluid between concentric spheres that rotate about the same axis with different angular velocities. If the inner sphere is held fixed while the outer one rotates, shear layers form on the cylinder $C$, tangent to the inner sphere and coaxial with the rotation vector. On the basis of a linear theory one expects shear layers on cylinder $C$ whenever the differential rotational of the spheres is small (provided the separation of the spheres is sufficiently large). It would be interesting to simulate such a regime numerically and then to decrease the angular velocity of the outer sphere until the shear layers on cylinder $C$ disappear and a radial equatorial jet forms, as in the laboratory experiments of *Bowden and Lord* [1963].

In the laboratory model of *Baker and Robinson* [1969] the working fluid fills the volume enclosed by two concentric rotating spheres and a cylinder $D$, the axis of which may be at any angle to the basic rotation vector. The wall of the model ocean basin is thus circular. Differential motion is due to the inner spherical cup rotating about the axis of the cylinder $D$. When the equator

passes through the basin, a zonal equatorial current that has a direction opposite to the longitudinal component of the surface forcing velocity is observed. For low Rossby numbers the current reverses when the direction of the driving reverses. As the Rossby number increases, the eastward undercurrent remains stable but the westward undercurrent becomes unstable. For the experiments conducted thus far, the horizontal Coriolis terms are important in the dynamics of the equatorial current (see section 3*a*).

Westward winds cause eastward flow at all depths at the equator in the model of *Bryan and Cox* [1968]. This presumably happens because the eastward pressure force is sufficiently large to cause eastward surface flow in the face of westward winds. (The same happens in *Charney*'s [1960] model for sufficiently large Rossby numbers. *Taft et al.* [1973] have observed such an occurrence.) The eastward equatorial current is a nonlinear shear layer in which the horizontal diffusion of momentum is important. It is probably the nonlinear counterpart of the shear layer studied by *Gill* [1971] (see section 3*a*).

## 3. REVIEW OF THEORIES

Let the angles of latitude and longitude be denoted by $\theta$ and $\varphi$, respectively, and let $r$ be the radial coordinate. If we confine attention to regions close to the equator, it is convenient to introduce the Cartesian coordinates $x$, $y$, and $z$, which measure distances westward from an eastern coast, northward from the equator, and upward from the ocean surface, respectively. We nondimensionalize these coordinates with respect to $L$, $L$, and $H$, where $L$ is a typical horizontal scale and $H$ is the depth of the ocean or the separation of the spheres in a laboratory apparatus. Let $u$, $v$, and $w$ be the associated velocity components and nondimensionalize them with respect to $U_0$, $U_0$, and $HU_0/L$, where $U_0$ is a typical horizontal velocity scale. The other parameters on which the flow depends are the radius of the earth (or of one of the spheres in a laboratory apparatus) $R$, the basic rotation rate $\Omega$, the coefficients of vertical and horizontal eddy viscosity $\nu_v$ and $\nu_H$, and the intensity of wind stress $\tau_0$, which is, of course, related to $U_0$. In laboratory experiments, $\nu_v = \nu_H$. If the fluid is stratified, a typical apparent temperature difference $\Delta T$, the coefficients of thermal diffusivity $K_v$ and $K_H$, the coefficient of thermal expansion $\alpha$, and the gravitational acceleration $g$ also enter the problem. The vertical (radial) component of the Coriolis parameter will be denoted by $f$, and its latitude gradient will be denoted by $\beta$. It is useful to form the following nondimensional numbers:

Ekman numbers

$$E_v = \nu_v R/2H^2 L\Omega \tag{1a}$$

$$E_H = (\nu_H H^2/\nu_v L^2)E_v \tag{1b}$$

Rossby number

$$\epsilon = U_0 R/2L^2\Omega \tag{1c}$$

Aspect ratio

$$\lambda = HR/L^2 \tag{1d}$$

$$\gamma = \alpha g\, \Delta T HR/2L^2 U_0 \Omega \tag{1e}$$

$$\Gamma_1 = K_v L/U_0 H^2 \tag{1f}$$

$$\Gamma_2 = \Gamma_1 (K_H/K_v)(H^2/L^2) \tag{1g}$$

It will be assumed that $E_v \ll 1$ and $E_H \ll 1$. If we confine attention to a region close to the equator ($L < R$), if we denote by $T$ the apparent temperature, nondimensionalized with respect to $\Delta T$, and if we neglect the viscous and nonlinear terms in the vertical momentum equation, the equations expressing conservation of mass, momentum, and heat (assumed to be valid in Boussinesq form) can be written as follows:

$$-E_v u_{zz} - E_H(u_{xx} + u_{yy}) + \epsilon(uu_x + vu_y + wu_z) + yv - \lambda w + P_x = 0 \tag{2a}$$

$$-E_v v_{zz} - E_H(v_{xx} + v_{yy}) + \epsilon(uv_x + vv_y + wv_z) - yu + P_y = 0 \tag{2b}$$

$$\lambda u - \gamma T + P_z = 0 \tag{2c}$$

$$u_x + v_y + w_z = 0 \tag{2d}$$

$$-\Gamma_1 T_{zz} - \Gamma_2(T_{xx} + T_{yy}) + uT_x + vT_y + wT_z = 0 \tag{2e}$$

*a. Wind-driven homogeneous models.* In this section we review theories that neglect density gradients so that equation 2*e* is irrelevant and (2*c*) can be simplified by putting $\gamma = 0$. If the motion is wind driven, choose $U_0 = \tau_0(R/2\Omega L\nu_v)^{1/2}$. The nondimensionalized horizontal velocities in the extraequatorial Ekman layer are then $O(1)$. We confine our attention to systems that are weakly diffusive and that have small Ekman numbers.

The homogeneous models can be subdivided into the following groups: (1) shallow linear models, (2) deep linear models, and (3) shallow nonlinear models. For the models in the first group, the driving is sufficiently weak for the flow to be linear everywhere, and the separation of the spheres is sufficiently small for the horizontal Coriolis terms to be negligible everywhere; the conditions of equation 3 are satisfied. For this parameter range the Ekman layers on the spheres merge at a distance $O(E_v L)$ from the equator, so that the vertical (radial) diffusion of momentum is important at all depths at the equator. It is possible for the vertical diffusion of momentum to be confined to thin boundary layers on the spheres, even at the equator, provided either that the depth of the model ocean is such that the horizontal Coriolis terms are important (the second group of models), or that the intensity of the driving is such that the nonlinear advection of momentum is important equatorially (the third group of models). The different cases will now be discussed in turn.

The simplest flow pattern realizable between concentric rotating spheres is axisymmetric and occurs when

$$\lambda^{1/2} < E_v \Rightarrow H < (\nu_v^2 R/4\Omega^2)^{1/5} \tag{3a}$$

$$\epsilon^{2/5} < E_v \Rightarrow \tau_0 < \nu_v^3 R/2H^5\Omega \tag{3b}$$

The appropriate equations are $2(a\text{–}e)$ with $E_H = \epsilon = \lambda = 0$. Under conditions $3(a, b)$, viscous effects are confined to Ekman layers of thickness $H(E_v/\sin\theta)^{1/2}$ on the bounding spheres. The stresses in the Ekman layers are comparable, and their meridional transports are equal and opposite. In the inviscid region between the Ekman layers the flow is azimuthal and radial; fluid is transferred from the Ekman layer on the slower rotating sphere to the one on the faster rotating sphere. The return flow from the faster to the slower sphere occurs in an equatorial boundary layer of width $O(\nu_v R/2\Omega H^2)$ $(= E_v L)$, where the Ekman layers, the depth of which increases as the equator is approached, merge. It follows that the radial (vertical) diffusion of momentum is important at all depths at this distance from the equator. The dynamics of this $O(E_v)$ boundary layer, in which the velocity components attain their highest values, have been investigated by *Stommel* [1960] and *Felzenbaum* [1966].

The effect of meridional barriers on the flow just described is dramatic (and well known). Away from the equator the Ekman layer on the inner sphere becomes of secondary importance. The azimuthal flow in the inviscid region, where there is now an $O(E_v^{1/2}U_0)$ meridional velocity component, becomes smaller by a factor of $O(E_v^{1/2})$ than the flow in the Ekman layer on the outer sphere. If the curl of the wind stress is nonzero, the asymmetric circulation is characterized by a dissipative western boundary layer. The dynamics of the $O(E_v L)$ equatorial boundary layer where the Ekman layers merge remain unchanged except for a constant $O(\tau_0/H)$ zonal pressure gradient. In this boundary layer the flow depends on local wind conditions only, and zonal variations appear implicitly through the boundary conditions. The azimuthal velocity at the equator, determined by a balance between (vertical) viscous stresses and the constant zonal pressure gradient, has a parabolic profile and does not reverse at any depth. (The reversal of the current in the models of *Stommel* [1960] and *Neumann* [1960] is a consequence of the arbitrary assumption that the vertically integrated zonal transport at the equator is zero. Note that a steady state is impossible in a closed basin if lateral friction is neglected and if the bottom is assumed to be slippery.) The net eastward transport of the $O(E_v)$ equatorial boundary layer returns westward in a more diffuse bottom frictional boundary layer of width $O(\nu_v RL^2/2\Omega H^2)^{1/3}$ $(=E_v^{1/3}L)$ [*Philander*, 1971*a*]. This frictional boundary layer, in which the flow is not a function of local wind conditions only and in which the stress in the bottom Ekman layer is comparable to that in the surface Ekman layer, effects a smooth transition from the extraequatorial flow to the equatorial flow, where friction is important at all depths.

If the ocean is sufficiently shallow for condition $3a$ to be satisfied, the velocity components are independent of the depth (radial) coordinate at latitudinal angles larger than $O(E_v)$. That this is a modification of the Proudman-Taylor theorem can be shown as follows. The momentum equations for the region between the Ekman layers are

$$yv - \lambda w + P_x = 0 \qquad -yu + P_y = 0 \qquad \lambda u + P_z = 0$$

These equations, together with the continuity equation, imply that the dependent coordinates are functions of $x$ and $\xi$ only where $\xi = z - y^2/2\lambda$. Lines on which $\xi$

has a constant value are parallel to the rotation vector (within the limits of the various approximations made). It follows that the dependent coordinates, and in particular the horizontal velocity components, are independent of the coordinate measuring distance parallel to the rotation vector. This is, of course, the Proudman-Taylor theorem. If the separation of the spheres is sufficiently small for (3*a*) to be satisfied, it follows that $\lambda \ll 1$, so that $\xi$, and therefore the dependent variables, are independent of $z$ at latitudinal angles greater than $O(E_v)$. From a geometrical point of view, (3*a*) permits us to approximate lines parallel to the rotation vector with radial lines. From a mathematical point of view, (3*a*) permits us to neglect the horizontal Coriolis terms (those multiplied by $\lambda$ in equations 2). *Carrier* [1965] calculated the effects of these terms as a first-order perturbation on the zeroth order flow described in the previous paragraph and found that they can cause a reversal of the zonal current at the equator.

If the separation of the spheres should be increased to the point where (3*a*) is violated, so that

$$\lambda^{1/2} \gg E_v \Rightarrow H \gg (\nu_v^2 R/4\Omega^2)^{1/5} \tag{4}$$

axial lines must be distinguished from radial lines everywhere (the horizontal Coriolis terms are no longer negligible), and the cylinder $C$, which circumscribes the inner sphere and which has generators parallel to the rotation vector, becomes a surface separating regions of different flow properties. (The surface $C$ is inside the $O(E_v)$ diffusive layer and is not of any significance when condition 3*a* is satisfied.) The axisymmetric flow inside $C$ for the parameter range (4) is similar to that discussed earlier except that 'radial' must be replaced by 'axial' in the description. The axisymmetric flow outside $C$, when condition 4 is satisfied and when relative motion is due to differential rotation of the spheres, is simply rigid body rotation with the angular velocity of the outer sphere [*Proudman*, 1956]. Shear layers on $C$ now play the role formerly performed by the $O(E_v L)$ equatorial boundary layer; they transfer fluid from the Ekman layer on the faster rotating sphere to the Ekman layer on the slower rotating sphere [*Stewartson*, 1966]. The depth of the Ekman layer on the inner sphere increases as the equator is approached until it reaches a thickness of $O(\nu_v^2 R/4\Omega^2)^{1/5}$ at a latitudinal angle that is $O(\nu_v/2\Omega R^2)^{1/5}$ [*Stewartson*, 1966; *Philander*, 1971*b*]. The radial diffusion of momentum is thus important only in thin boundary layers on the spheres, even at the equator.

The presence of meridional barriers affects this axisymmetric flow in the following manner. As for the parameter range (3), the highest velocities inside $C$ are attained in the Ekman layer on the driving surface (the outer sphere, say) and in a western boundary current. There is no transport across $C$ except in the Ekman layer on the outer sphere. The transport of this Ekman layer converges on the equator, thus giving rise to an eastward equatorial current of width $O(\nu_v/2\Omega R^2)^{1/7}$ radians and depth $O(\nu_v^2 R H^2/4\Omega^2)^{1/7}$. This current feeds an eastern boundary current outside $C$ that is linked up with the western boundary current inside $C$ by westward flow in shear layers on $C$ (see Figure 15). At the equator the direction of the deep flow is opposite to that of the surface flow [*Philander*, 1972].

The horizontal Coriolis terms are important in the dynamics of the under-

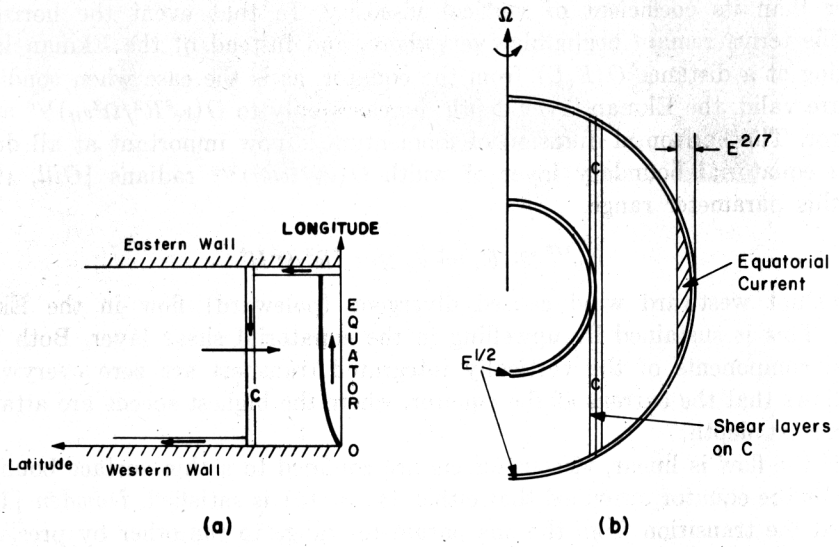


Fig. 15. (*a*) Flow pattern from above for the parameter range (4). (*b*) The boundary layers in a plane containing the axis of rotation.

current observed in the experiments of *Baker and Robinson* [1969] (see section 2*f*). For the cases on which they report, the separation of the spheres, although sufficiently large for the cylinder $C$ to be important, is also sufficiently small for the width of the shear layers on $C$ to be comparable to the depth of their 'ocean.' If this is taken into consideration, it is possible to explain some of Baker and Robinson's measurements, namely, those corresponding to a linear parameter range [*Philander*, 1972].

If the depth of the ocean is assumed to be 5 km, the cylinder $C$ intersects the ocean surface near 2.5° latitude. Although the horizontal Coriolis terms, and thus the cylinder $C$, are unimportant in the surface layers and do not affect the dynamics of the undercurrent, it has not been established that these terms are negligible below the surface layers. According to the theoretical results of *Kozlov* [1967], the horizontal Coriolis terms are important at the equator below a depth of about 500 meters. Measurements in the deep equatorial waters and further theoretical investigations of the effect of weak stratification on the flow discussed in the above paragraphs are necessary to clarify the role of the horizontal Coriolis terms in the dynamics of the deep equatorial currents. A study of stratified rotating flow when the rotation vector is perpendicular to gravity will be particularly valuable.

Changing the parameter range from that given by (3) to that given by (4) transforms the western boundary layer (inside $C$) from one in which dissipation in the bottom Ekman layer is important [*Stommel*, 1948] to one in which diffusion of vorticity into the vertical wall (western boundary) is important [*Munk*, 1950]. This transformation can also be effected without increasing the separation of the spheres but by replacing the fluid with a hypothetical fluid that has a coefficient of lateral (eddy) viscosity $\nu_H$ that is much

larger than its coefficient of vertical viscosity. In that event the horizontal Coriolis terms remain negligible everywhere, and instead of the Ekman layers merging at a distance $O(E_v L)$ from the equator, as is the case when conditions (3) are valid, the Ekman layer depth increases only to $O(\nu_v^3 R^2/\Omega^2 \nu_H)^{1/6}$ at the equator. The horizontal diffusion of momentum is now important at all depths in an equatorial boundary layer of width $O(\nu_H/\Omega R^2)^{1/3}$ radians [*Gill*, 1971]. For this parameter range,

$$E_H^{1/3} \gg E_v \Rightarrow \nu_H \gg \nu_v^3 R^2/\Omega^2 H^6 \tag{5}$$

a constant westward wind caused divergent (poleward) flow in the Ekman layer. This is sustained by upwelling in the equatorial shear layer. Both horizontal components of the vertically integrated transport are zero everywhere. It follows that the current at the equator, where the highest speeds are attained, reverses at depth.

If the flow is linear, viscous effects are confined to a thin surface boundary layer at the equator, provided that either (4) or (5) is satisfied. *Dowden* [1972] studied the transition from the one parameter range to the other by presenting solutions, in closed form, to the boundary layer problem in which both lateral friction and the horizontal Coriolis terms are important at the equator.

We next turn our attention to the modifications of the flow corresponding to the parameter range (3) when the nonlinear advection of momentum is taken into consideration. According to the linear theory for the parameter range (3), the flow at the equator is in the same direction at all depths. *Robinson* [1966] calculated the first-order correction due to nonlinearities and found that, irrespective of the direction of the zonal wind, the correction terms always correspond to eastward flow. Thus, for sufficiently large Rossby numbers, the flow at depth at the equator is eastward even when the wind stress is westward. This result remains valid when the Rossby number is too large for an expansion procedure to be valid; *Charney*'s [1960] calculations show eastward flow at depth when the surface winds are westward and when the Rossby number is such that

$$\epsilon^{2/5} \gtrsim E_v \Rightarrow \tau_0 \gtrsim \nu_v^3 R/2H^5\Omega \tag{6}$$

If these conditions are satisfied, both the vertical diffusion and the nonlinear advection of momentum are important at all depths at a distance $O(\tau_0^2 R^3/8\Omega^3\nu_v)^{1/5}$ $(= \epsilon^{2/5}L)$ from the equator. The zonal velocity component at the equator is $O(R\tau_0^4/2\nu_v^2\Omega\nu_v^2)^{1/5}$. If we choose the depth $H$, the depth of the homogeneous layer, to be $1.5 \times 10^4$ cm, and if we choose appropriate oceanic values for the other parameters, we find that the value $\nu_v = O(10\ \text{cm}^2\ \text{sec}^{-1})$ gives scales that are in reasonable agreement with measurements of the undercurrent in the mixed layer of the Western Pacific. One arrives at about the same value for $\nu_v$ by assuming that at the core of a symmetric undercurrent the zonal pressure gradient is balanced by the vertical diffusion of momentum. This assumption gives the approximate value 5 $\text{cm}^2\ \text{sec}^{-1}$ for $\nu_v$ [*Wyrtki and Bennet*, 1963; *Knauss*, 1966]. For the fields to have smooth latitudinal derivatives at the equator, an equatorial shear layer in which lateral friction is important

is necessary. Unless the value of $\nu_H$ exceeds $O(10^8$ cm$^2$ sec$^{-1})$, this shear layer is of secondary importance. If $\nu_v$ is $O(10$ cm$^2$ sec$^{-1})$ and if $\nu_H$ is smaller than $O(10^8$ cm$^2$ sec$^{-1})$, on substitution of appropriate values for the oceanic parameters one finds that conditions 6 rather than the conditions corresponding to other parameter ranges are satisfied. It follows that the model under discussion is the one that is relevant to the motion observed in the homogeneous surface layer at the equator in the western Pacific. In this model the zonal pressure gradient retains its constant $O(\tau/H)$ extraequatorial value at the equator. The $O(\epsilon^{2/5})$ equatorial current depends on local wind conditions only and is embedded in a more diffuse boundary layer of width $O(E_v^{1/3}L)$. This boundary layer is responsible for returning the net eastward transport of the equatorial current westward. These two currents form an essentially closed system. Circulation patterns for various types of wind stresses have been described by *Philander* [1971*a*]. Whereas *Charney*'s [1960] calculations are for the flow in the equatorial plane only, calculations of *Charney and Spiegel* [1971] give the meridional structure of the flow. One of Charney and Spiegel's most interesting results, anticipated by *Robinson* [1966], is the upwind displacement of the core of the undercurrent when the winds have a meridional component. This is in response to the meridional pressure gradient set up by the wind [*Gill*, 1972].

In the two-dimensional model of *Charney and Spiegel* [1971], the fields develop cusps at the equator for sufficiently large Rossby numbers (see Figure 4). The explanation for this is that particles coming from either side of the equator tend to conserve their absolute vertical vorticity component and thus arrive at the equator with a relative vorticity equal to that of the earth at the latitude of origin [*Fofonoff and Montgomery*, 1955]. It is unlikely that vorticity will be conserved if friction is important at all depths. One concludes that an increase in the Rossby numbers causes the vertical diffusion of momentum to be confined to a thin surface boundary layer, even close to the equator. A scale analysis reveals that if $\tau_0 \gg \nu_v^3 R/2\Omega H^5$, the depth of the nonlinear equatorial Ekman layer is $O(R\nu_v^3/2\Omega\tau_0)^{1/5}$ [see also *Pushistov*, 1970]. Below this boundary layer the zonal but not the meridional flow is in geostrophic balance. The calculations of *Leishman* [1967] confirm that this happens when the Rossby number becomes large.

The presence of cusps in the model of *Charney and Spiegel* [1971] has another implication, namely, that shear layers are present at the equator when the vertical diffusion of momentum is confined to thin surface boundary layers. Because of the absence of lateral friction from the Charney and Spiegel model, the discontinuous meridional derivatives become infinite for sufficiently large Rossby numbers, at which stage the numerical iterations diverge. This happens for lower Rossby numbers for an eastward than for a westward wind. The situation is remedied by the inclusion of lateral friction [*McKee*, 1973]. Unlike the shear layers that arise when the parameter range corresponds to (5), the layers under discussion here can occur in a laboratory situation. If a sphere is rotated in an otherwise stationary fluid, the boundary layer on the sphere erupts in a radial jet at the equator [*Bowden and Lord*, 1963]. It is likely that

the meridional diffusion of momentum is important in the jet. *Stewartson* [1958] disagrees, asserting that the width of the shear layers at the equator is much less than that of the jet. His analysis does not take into consideration that the thickness of the boundary layer on the sphere may increase as the equator is approached and may be singular at the equator. (The thickness of a linear Ekman layer for example, is proportional to $(\nu_v/\sin\theta)^{1/2}$ and increases rapidly as the equator is approached.) This problem requires further study.

*b. Stratified models.* The oceanic motion due to density gradients when the winds have temporarily died down is a much-studied problem in connection with the thermocline. All the known solutions that are valid away from the equator have equatorial singularities. Physically, this manifests itself in a convergence of fluid at the equator. In the introduction we demonstrated how this can be inferred from the observed density field. This convergence can, alternatively, be deduced in the following manner. The linear flow away from the equator satisfies the vorticity equation

$$\beta v = f w_z \tag{7}$$

If the vertical velocity at the base of the thermocline is upward (positive) and if the wind-induced Ekman layer flow is convergent, so that the Ekman layer suction $w_E$ is negative, which is usually the case in the tropics, it follows from the integration of (7) across the thermocline that the meridional transport in the thermocline $V$ is equatorward in both hemispheres

$$V = \int v\, dz = -\frac{f}{\beta}(w_\infty - w_E)$$

Since an eastward pressure force is associated with the slope of the isotherms, upward from west to east in the tropics, the equatorial convergence gives rise to an eastward current at the equator. The characteristic scales of this current may be determined by a scale analysis, which must take into consideration that certain physical processes that are negligible away from the equator are important at the equator. Observations indicate that although the downstream flow in the undercurrent may be in geostrophic equilibrium, the importance of the nonlinear advection of zonal momentum prevents the meridional flow from being in geostrophic equilibrium close to the equator. The scaling that reflects this is the following: width, $\sim(\alpha g \Delta T H R^2/4\Omega^2)^{1/4}$; downstream velocity, $\sim(\alpha g \Delta T H)^{1/2}$; cross-stream velocity, $\sim(\alpha^3 g^3 \Delta T^3 H^3/4\Omega^2 R^2)^{1/4}$; vertical velocity, $\sim(\alpha g \Delta T H^3/R^2)^{1/2}$. The depth $H$ of the undercurrent has been taken to be that of the thermocline just outside the undercurrent. This is a reasonable assumption if the undercurrent is maintained by equatorward flow in the thermocline. It is, however, desirable that the depth of the undercurrent also be determined internally. This is possible, provided that the nature of the singularity of the solution to the extraequatorial flow is known and provided it is specified that there be a smooth transition from the equatorial to the extraequatorial region. If we take as the solution to the extratropical flow the one proposed by *Robinson and Welander* [1963] in which the vertical velocity has an equatorial singularity

of the type ($w \sim y^{-2/3}$), the appropriate scaling, now dependent on coefficients of eddy viscosity and diffusivity, is that shown in Table 1. The appropriate equations are (2*a–e*), with $\lambda = E_H = \Gamma_2 = 0$ and with (2*b*) reduced to a geostrophic balance. These equations describing flow in the equatorial thermocline were originally derived by *Robinson* [1960]. Because they are fully three-dimensional, they pose a formidable problem. There have been two attempts at isolating the flow at the equator. *Veronis* [1960] expands the dependent variables in a Taylor series in $y$ but finds that the resultant set of equations cannot be closed; there are more unknowns than equations. To obtain a closed set, Veronis assumes that the dependent variables other than $T$ and $p$ are independent of $x$ ($T$ and $p$ are taken to be linear functions of $x$) and writes $w = W + w'$ where $W$ is a constant and $|w'| \ll |W|$. The solution obtained in this manner is at best a very approximate one, because the boundary condition that the vertical velocity is zero at the surface implies that $|w'| = |W|$ on that surface. *Krivelevitch* [1968] isolates the flow in the equatorial plane in an effective but unacceptable manner: he assumes that the equatorial plane is a plane of symmetry ($v = 0$, which is a reasonable assumption) and disregards all terms in which meridional derivatives appear ($\partial/\partial y = 0$, an unreasonable assumption, especially in the continuity equation). The problem solved is that corresponding to nonrotating, two-dimensional (in $x$ and $z$) flow between two horizontal surfaces; a stress is applied at the upper surface, which is also heated.

*Philander* [1973] retained the three-dimensionality of the problem in a two-dimensional framework by eliminating explicit zonal variations by means of a similarity transformation. The motivation for this is the absence of an intrinsic zonal scale for the undercurrent. Thus profiles at various longitudes look, apart from an apparent stretching of the coordinates, very similar [see *Knauss*, 1966,

TABLE 1. Scaling for the Equatorial Thermocline

| Parameter | | Vertical Eddy Viscosity, Coefficient Values | | |
|---|---|---|---|---|
| | | $\nu_v = 1$ | $\nu_v = 10$ | $\nu_v = 100$ |
| Width, cm | $\left(\frac{\alpha^2 g^2 \Delta T^2 \nu_v^3 L R^5}{\Omega^5 K_v^2}\right)^{1/10}$ | $1.8 \times 10^7$ | $2.2 \times 10^7$ | $2.8 \times 10^7$ |
| Depth, cm | $\left(\frac{\nu_v K_v R^2}{\alpha g \Delta T}\right)^{1/5}$ | $0.28 \times 10^4$ | $0.7 \times 10^4$ | $17 \times 10^4$ |
| Zonal velocity, cm/sec | $(\alpha^2 \Delta T^2 g^2 K_v^3 L/\nu_v^2)^{1/5}$ | 80 | 100 | 125 |
| Meridional velocity, cm/sec | $\left(\frac{\alpha^6 g^6 \Delta T^6 K_v^4 R^5}{\Omega^5 L^7 \nu}\right)^{1/10}$ | 10 | 21.8 | 43 |
| Vertical velocity, cm/sec | $\left(\frac{\alpha g \Delta T K_v^4}{\nu_v L^2}\right)^{1/5}$ | $8 \times 10^{-4}$ | $31.3 \times 10^{-4}$ | $125 \times 10^{-4}$ |

The orders of magnitude of various fields are shown for various values of vertical eddy viscosity (cm²/sec). The Prandtl number has been taken to be 1.

Figure 3]. The similarity transformation is effected by writing

$$u(x, y, z) = x^{-2\alpha}\mu(\eta, \zeta) \tag{8a}$$

$$w = x^{-2\alpha-\beta-1}\omega(\eta, \zeta) \tag{8b}$$

$$v(x, y, z) = x^{-3\alpha-1}\nu(\eta, \zeta) \tag{8c}$$

$$T = x^{-4\alpha+\beta}\theta(\eta, \zeta) \tag{8d}$$

where

$$\eta = x^{\alpha}y \tag{8e}$$

$$\zeta = x^{\beta}z \tag{8f}$$

The constants $\alpha$ and $\beta$ are determined by the surface boundary conditions and by the influx conditions at some extraequatorial latitude. If we want lines of constant density to slope upward from west to east, even when the sea surface temperature is constant, it is necessary that we choose $\beta < 0$. (The coordinate system is a left-handed one; $x$ measures distance from an eastern wall.) For the sea surface temperature to increase from east to west, it is necessary that $4\alpha < \beta < 0$. These inequalities imply that the undercurrent, a surface current when the winds temporarily abate, becomes slower, narrower, and shallower downstream. Since it is maintained by an influx of fluid from the sides, the conservation of mass requires that there be equatorial downwelling. Whereas it is possible for the thermocline away from the equator to be maintained by a balance between the downward diffusion of heat and upward advection of cold water, maintenance by this means is not possible at the equator, where the two processes transmit heat in the same direction (downward). An advection of heat from colder regions is necessary. Since isotherms slope upward from west to east, a deep westward equatorial current is implied.

In the next section we discuss the effect of local winds on the flow described above.

## 4. A WIND-DRIVEN STRATIFIED MODEL

The motion described in the previous section (3*b*) occurs when the local winds temporarily die out while the density gradients, caused by the long-term averaged winds, persist. The modification of the flow due to variations in the intensity and direction of the local winds will now be studied. The long-term averaged winds, as reflected in the longitudinal gradient of the sea surface temperature, will be the same for all the cases on which we report.

Attention will be confined to solutions that permit a similarity transformation (8) of the equations, since such a transformation effects considerable mathematical simplifications. Unfortunately, the simplifications are accompanied by severe restrictions on the class of solutions that can be generated and on the possible boundary conditions that can be imposed. For example, it is not possible to check whether this model adequately simulates the observed flow; such a check requires that the observed sea surface temperature and surface winds be given,

that the observed mass and heat flux at two extratropical latitudes (6°N and 6°S, say) be given and that the model be used to simulate the flow observed under those conditions. It is unlikely that the boundary conditions will conform to the similarity transformation (8). A genuinely three-dimensional model is necessary to remove the limitation to which the present model is subject. Thus, even though the zonal variations of the undercurrent predicted by the similarity transformation (8) are in agreement with the observations at certain longitudes (see section 2*b*), the present model and the results to be presented here must be regarded as precursory.

If we nondimensionalize the variables by taking as the basic scales those given in Table 1 and if we perform the similarity transformation (8), the equations describing flow in the extraequatorial thermocline can be written as follows:

$$-\mu_{\zeta\zeta} - \Gamma\mu_{\eta\eta} - (5\alpha + \beta)\mu^2 + (\bar{v}\mu)_\eta + (\bar{\omega}\mu)_\zeta + \eta v - 4\alpha\pi + \alpha\eta\pi_\eta + \beta\zeta\pi_\zeta = 0 \quad (9a)$$

$$\epsilon'[-v_{\zeta\zeta} - \Gamma v_{\eta\eta} - (2\alpha + \beta - 1)\mu v + (\bar{v}v)_\eta + (\bar{\omega}v)_\zeta] - \eta\mu + \pi_\eta = 0 \quad (9b)$$

$$-\theta + \pi_\zeta = 0 \quad (9c)$$

$$-(3\alpha + \beta)\mu + \bar{v}_\eta + \bar{\omega}_\zeta = 0 \quad (9d)$$

$$-\theta_{\zeta\zeta} - \Gamma\theta_{\eta\eta} - 7\alpha\mu\theta + (\bar{v}\theta)_\eta + (\bar{\omega}\theta)_\zeta = 0 \quad (9e)$$

where

$$\bar{v} = v + \alpha\eta\mu \qquad \bar{\omega} = \omega + \beta\zeta\mu$$

$$\epsilon' = (\nu_v{}^3R^5\alpha^2g^2\Delta T^2/\Omega^5L^9K_v{}^2)^{1/5} \qquad \Gamma = \frac{\nu_H}{\nu_v}(\Omega^5K_v{}^3/RL\alpha^4g_4{}^4T^4)^{1/5}$$

The appropriate boundary conditions are the following

$$\theta = 1 \quad \mu_\zeta = c_1\tau^x \quad v_\zeta = c_2\tau^y \quad \omega = 0 \quad \text{at} \quad \zeta = 0 \quad (10a)$$

$$\mu_\zeta = v_\zeta = \theta = \omega + \zeta_0\mu \quad \text{at} \quad \zeta = -\zeta_0 \quad (10b)$$

The nondimensional constants $c_1$ and $c_2$ in (10*a*) have the values

$$c_1 = \tau_0(K_vR^2/\nu_v{}^5L\alpha^3g^3\Delta T^3)^{1/5} \qquad c_2 = \tau_0(\Omega^5L^7K_v/\nu_v{}^{10}R\alpha^8g^8\Delta T^8)^{1/10}$$

so that all the variables in (10) are nondimensional. If we choose $\nu_v = K_v = 10$ cm$^2$ sec$^{-1}$, the unit for the nondimensional wind stress $\tau^x$ is $\frac{1}{7}$ cm$^2$ sec$^{-2}$. Note that all the numbers in Figures 16, 17, and 18 are nondimensional. The above is the basic unit for the wind stress; the other units are given in Table 1.

It is necessary that the influx of mass, heat, and momentum at large values of $|\eta|$ be given. The scaling shown in Table 1 is based on the assumption that the equatorial solutions merge smoothly with the extraequatorial solutions of *Robinson and Welander* [1963]. Thus the boundary conditions at large values of $|\eta|$ must be solutions to the extraequatorial thermocline equations. The method usually used to solve those equations needs to be modified slightly because the surface is not stress free. We assume that the flow in the extraequatorial Ekman layer is linear and that the depth of that layer is much smaller than that of the thermocline, so that the temperature is a constant in the Ekman layer. Solutions can then be found analytically. In particular, a value for the vertical velocity $w$

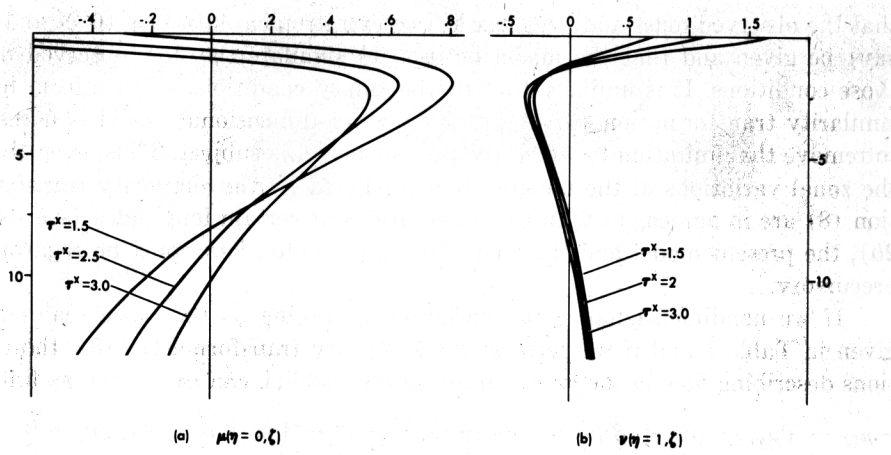


Fig. 16. (*a*) The zonal velocity profile at the equator and (*b*) the meridional velocity at $\eta = 1$ for various values of the wind stress.

at the base of the Ekman layer can be obtained. This value is used as the surface boundary condition in solving the extraequatorial thermocline equations numerically.

The method of solution for equations 9(*a–e*) subject to boundary conditions 10(*a*, *b*) is given in the appendix. The values of the following parameters remain the same for all the cases to be considered:

$$\alpha = -0.037 \qquad \beta = 0 \qquad \zeta_0 = 15 \qquad \Gamma = 0.75 \qquad \epsilon' = 0.2$$

The zonal variations implied by these values can be inferred from (8). The consequences of varying some of these parameters have been discussed elsewhere [*Philander*, 1973].

The choice of a nonzero value for $\epsilon'$ enables us to specify the wind stress and sea surface temperature independently. When we investigated the case in which the ocean surface is stress free (see section 3*b*), we put $\epsilon' = 0$ and chose a sea surface temperature with no latitudinal gradient (thus satisfying (9*b*) at the surface $\zeta = 0$). It is possible to have $\epsilon' = 0$ and to impose stress boundary conditions at the surface at the equator, provided that the (nondimensional) stress is $O(1)$ and provided that the latitudinal gradient of the sea surface temperature is consistent with the thermal wind equation. Thus, for sufficiently weak winds, the downstream flow of the undercurrent is in geostrophic balance. If the strength of the wind should increase so that the nondimensional stress is much larger than 1, a nonlinear equatorial Ekman layer of depth $O(R\nu_v^3/2\Omega\tau_0)^{1/5}$ (see section 3*a*) is formed. In this boundary layer the terms multiplied by $\epsilon'$ in (9*b*) are important. In the thermocline below that boundary layer the zonal flow is in geostrophic balance. The depth of the nonlinear equatorial Ekman layer is inversely proportional to the wind strength. It follows that if conditions are symmetric about the equator, the zonal flow of the undercurrent is always in geostrophic balance irrespective of the strength of the wind. Either cross-equatorial winds or zonal winds with a horizontal shear are necessary for ageostrophy.

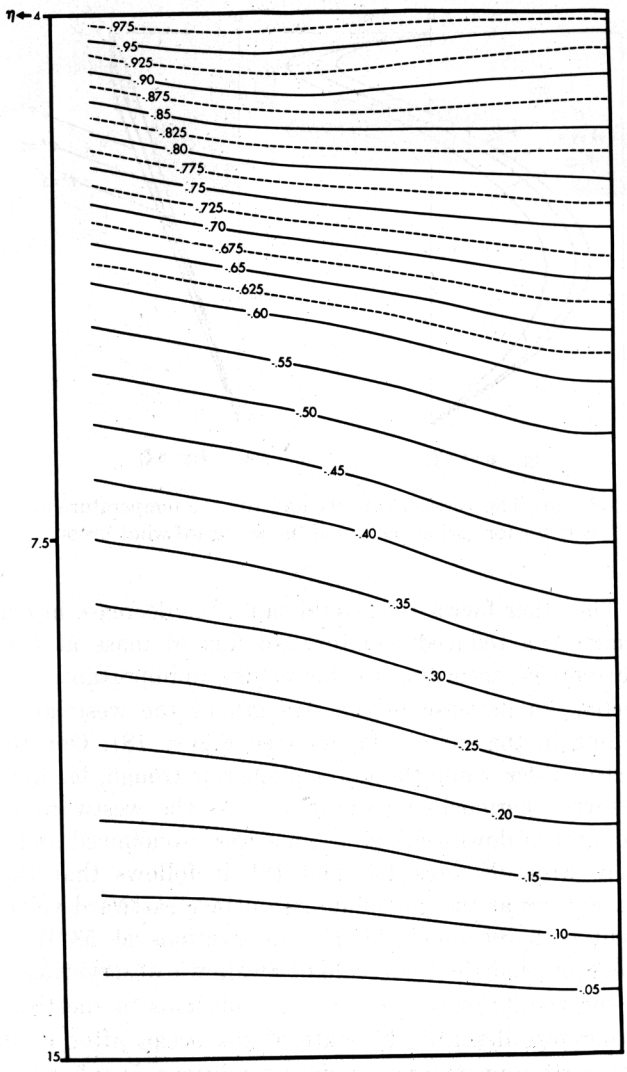


Fig. 17. Isotherms in a meridional plane for $\tau^x = 3$.

*a. Symmetric conditions.* In the temporary absence of local winds, the meridional circulation of the eastward surface jet at the equator is characterized by downwelling. Westward winds cause the surface flow to be westward, so that the eastward core becomes subsurface. It is evident from Figure 16*a* that the intensity of the westward surface current is proportional to that of the westward winds. Increased frictional dissipation causes the maximum eastward velocity to decrease as the westward winds grow in strength. Figure 16*b* shows that changes in surface wind conditions hardly affect the meridional flow below the surface layers. This seems to suggest that, when the transport of the undercurrent decreases as the winds increase in intensity, upwelling causes a loss of fluid from the undercurrent to the westward South Equatorial Current, in which there is a

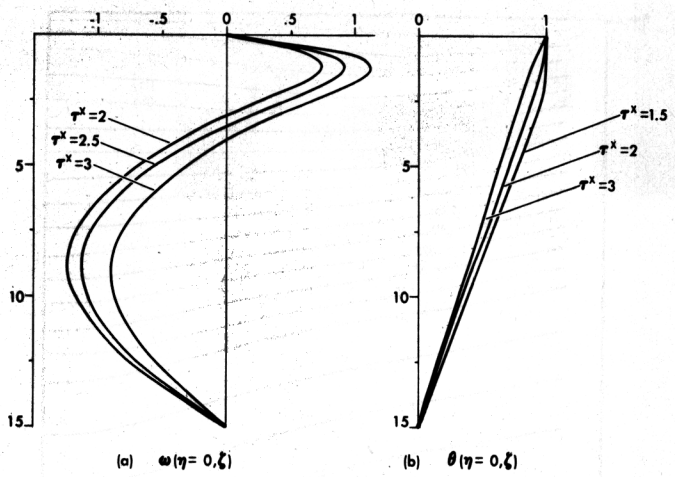


Fig. 18. (*a*) The vertical velocity and (*b*) the temperature at the equator for various values of the westward wind stress.

poleward drift. The other factor that could cause the decrease in transport of the undercurrent, namely a reduced equatorward flux of mass at the level of the core of undercurrent, is, according to this model, unimportant.

As is expected, an increase in the strength of the westward winds causes increased upwelling in the surface layers (see Figure 18). One thus finds that the upper isotherms ridge while the lower isotherms trough, leading to a spreading of the equatorial thermocline (Figure 17). As the westward winds grow in intensity, the equatorial downwelling becomes less pronounced and the upwelling more pronounced. From Figures 16*a* and 18*b* it follows that the depth of a given isotherm increases as the maximum subsurface eastward velocity increases. This is consistent with *Swallow*'s [1967] observations at 58°W in the Indian Ocean. Note, however, that the time scale of Swallow's observations was less than 1 day, whereas the results presented here are solutions to the time-independent equations and therefore describe the state of the ocean after it had come into equilibrium, with certain unchanging surface conditions. It takes the model about 10 days (if $\nu_v = 10$ cm$^2$ sec$^{-1}$) to adjust from a state corresponding to a wind $\tau^x = 2$ to a state corresponding to $\tau^x = 4$.

*b. Asymmetric conditions.* The constant-density model of *Charney and Spiegel* [1971] shows that a cross-equatorial wind causes an upwind displacement of the core of the undercurrent (see Figure 4). This is also true of the stratified model under discussion; it is found that the southward displacement increases as the intensity of the northward component of the wind increases. Whereas the most intense downwelling occurs at the equator when conditions are symmetric about the equator, the stratified model shows that the center of the region of convergence moves downwind, northward when the winds are from the south. This gives rise to a mild front a short distance from the equator. If the surface boundary condition (10) were changed so that the heat flux at

the surface rather than the sea surface temperature is given, it might be possible to obtain a sharp front with this model.

Another factor that may influence the position of the core of the undercurrent is the horizontal shear of the zonal winds at the equator. It is found that if the wind has no northward component and if the zonal component varies with latitude in such a manner that the wind south of the equator is more intense than the wind north of the equator, the core of the undercurrent is north of the equator.

## 5. DISCUSSION

We have, on several occasions, expressed reservations about the apparent success of the theories and models developed thus far. One of the reasons is that no allowance has yet been made for the interaction of the undercurrent with waves generated at the equator or propagating equatorward from higher latitudes. (For a review of the theoretical studies of the various waves trapped at the equator, the reader is referred to articles by *Moore* [1972] and *Gill* [1972].) Waves at the equator may be caused either by surface winds—the sudden onset of the westerlies over the eastern tropical Atlantic, the monsoons over the Indian Ocean and Western Pacific, or the four to five day oscillations of the winds over the Central Pacific [*Groves,* 1956; *Groves and Miyata,* 1967]—or by instabilities of some of the equatorial currents. These instabilities have received practically no theoretical attention [but see *Stone,* 1971] and may shed light on the cause of the peculiar mixed layers at the equator: the deep homogeneous surface layer in the Indian Ocean and Western Pacific and the subsurface mixed layer, the thermostad, in the eastern part of the Pacific and in the Atlantic (see Figure 12).

Recent measurements by *Taft et al.* [1973] at 150°W, 1°N at a depth of 102 meters show that the flow there has fluctuations with a 4- to 5-day periodicity. The winds in that region fluctuate with the same periodicity but not with the same phase. According to linear theories, winds with this frequency $w$ cause the Ekman layer to be singular (to 'erupt') at the latitude where $f = w$, or approximately 6°N and 6°S [*Greenspan,* 1968]. Unfortunately, there were no measurements at 150°W at those latitudes. *Holton et al.* [1971] have suggested that the location of the ITCZ in the atmosphere can be determined by this factor.

The measurements of *Swallow* [1967] at 0°, 54°E in the Indian Ocean show that the maximum eastward speed of the undercurrent, 100 ± 20 cm/sec, can go from the one extreme to the other extreme in a matter of hours. This seems to imply the presence of high-frequency waves and possibly of gravity waves. F. P. Bretherton and D. W. Moore (private communication, 1972) have investigated the possibility of internal gravity waves, generated extratropically, propagating equatorward and having their momentum absorbed by the undercurrent, which they thus sustain. Could this explain the presence of the undercurrent in the eastern Indian Ocean in September 1962, late in the southwest monsoon season? Another mechanism that deserves attention is the generation of gravity waves near the ocean surface at the equator. *Swallow* [1967] has commented on the vertical displacement of isotherms that accompanies the previously mentioned variations in the maximum eastward speed at the equator. This displacement

may be due to variable upwelling caused by variable winds. It is conceivable that the gravity waves thus generated propagate downward until they encounter a critical layer, where their phase velocity is equal to that of the current. Absorption of momentum in this layer may be the explanation for the deep secondary eastward maximum of the undercurrent observed on several occasions (see section 2*b* and Figure 8).

Not only the winds but also the tides can produce a vertical oscillation of isohalines. A spectral analysis of the 60-day current meter records from 0°N, 35°W in the late winter of 1963 show a marked 12.4-hour (tidal) periodicity [*Stalcup and Metcalf*, 1966]. *Rinkel* [1969] found that the high-salinity core of the Equatorial Undercurrent in the Atlantic oscillates in the vertical plane with the same frequency. The amplitude of the oscillation of the isohalines at the salinity maximum is about 9 meters. At greater depths, 360–480 meters, the amplitude is between 30 and 40 meters. In addition to oscillating in a vertical plane, there is also evidence that the salinity core undergoes meridional displacements. The salinity maps prepared by *Rinkel* [1969] show horizontal excursions of the salinity maximum of about 120 km in a period of approximately 14 days. These excursions may be associated with a meandering undercurrent, but there is at this time no evidence to support such a speculation.

## APPENDIX: METHOD OF SOLUTION FOR EQUATIONS 9

For the purpose of solving equations 9 numerically, it is expedient to convert the problem into a time-dependent one. Equations 9(*c*, *d*) remain unchanged, and the horizontal momentum equations and heat equation are affected in an obvious manner. Given initial values of the dependent variables, it is now possible to predict new values for $\theta$, $\mu_\zeta$, and $\nu_\zeta$ from the modified versions of equations 9(*e*, *a*, *b*), respectively. To obtain $\mu$ and $\nu$ we predict the vertically integrated zonal and meridional transports.

$$\int_{-\zeta_0}^{0} \mu \, d\zeta = \varphi_\eta \qquad \int_{-\zeta_0}^{0} \nu \, d\zeta = -\alpha\eta\varphi_\eta + (3\alpha + \beta)\varphi$$

from the following vorticity equation, which can be derived from (9*a*, *b*).

$$\begin{aligned}
\Phi_t = {} & \lambda\Gamma\Phi_{\eta\eta} - \lambda^2\Gamma(a + 4\epsilon'\alpha^2\eta)\eta\Phi_\eta + \lambda^3\Gamma[(\alpha + 4\epsilon'\alpha^2)(a + 2\epsilon'\alpha^2)\eta^2]\Phi \\
& - \lambda^4\Gamma(2a + 11\epsilon'\alpha^2 + 3\epsilon'\alpha\beta)\Phi - \beta\int_{-\zeta_0}^{0} \zeta\theta_\eta \, d\zeta + 3\alpha\epsilon'\tau^y - \epsilon'\alpha\eta\tau_\eta{}^y + \tau_\eta{}^x \\
& + \Gamma\eta\varphi_\eta\left[\frac{\alpha - \beta}{\Gamma} + 3a^2\lambda^2 + (9\epsilon'\alpha^2 + 3\epsilon'\alpha\beta)(2a + 4\epsilon'\alpha\beta)\lambda^2 + 6\epsilon'\alpha^2 a\lambda^2\right. \\
& \left. - \lambda^3 a(a + 4\epsilon'\alpha^2)(a + 2\epsilon'\alpha^2)\eta^2\right] \\
& - \Gamma\varphi\left\{\frac{3\alpha + \beta}{\Gamma} + \lambda^2(9\epsilon'\alpha^2 + 3\epsilon'\alpha\beta)\right. \\
& \left. \cdot[\eta^2\lambda(a + 4\epsilon'\alpha^2)(a + 2\epsilon'\alpha^2) - (2a + 11\epsilon'\alpha^2 + 3\epsilon'\alpha\beta)]\right\}
\end{aligned}$$

$$+\left[(5\alpha+\beta)\frac{\partial}{\partial\eta}-\alpha\frac{\partial^2}{\partial\eta^2}\eta\right]\int_{-\zeta_0}^{0}\mu^2\,d\zeta+\left(-3\epsilon'\alpha\frac{\partial}{\partial\eta}+\alpha\eta\frac{\partial^2}{\partial\eta^2}\right)\int_{-\zeta_0}^{0}\nu\,d\zeta$$

$$+\left[(-1+\epsilon'\alpha^2\eta^2)\frac{\partial^2}{\partial\eta^2}+3\alpha\epsilon'(5\alpha+\beta)-\alpha\epsilon'(7\alpha+1+\beta)\eta\frac{\partial}{\partial\eta}\right]\int_{-\zeta_0}^{0}\mu\nu\,d\zeta \tag{A1}$$

$$a=-\epsilon'\alpha(\beta+5\alpha)$$

$$\lambda=1/(1+\epsilon'\alpha^2\eta^2) \tag{A2}$$

$$\Phi=(1/\lambda)\varphi_{\eta\eta}-a\eta\varphi_\eta+3\alpha\epsilon'(3\alpha+\beta)\varphi$$

We obtain $\varphi$ by predicting $\Phi$ from (A1) and then solving the elliptic equation (A2). Alternatively, since we are interested in the steady state only, we can disregard the time-dependent term in (A1), substitute (A2) into (A1), and solve the resultant fourth-order equation for $\varphi$.

The iterations are continued until a steady state is reached. (Note that initially the temperature is assumed not to vary with latitude and to have its given extraequatorial value. We therefore do not have a state of rest initially.) An earlier paper [*Philander*, 1973] gives details of the finite difference scheme employed.

*Acknowledgments.* I am indebted to M. Hisard of the Office de la Recherche Scientifique et Technique Outre-Mer (Orstom), Abidjan, for making his French translations of various Russian papers available to me, and to Dr. R. G. Williams for bringing to my attention a number of papers of which I had been unaware.

The work was supported by the Geophysical Fluid Dynamics Laboratory of the National Oceanic and Atmospheric Administration under grant E22-21-70(G).

## REFERENCES

Akamatsu, H., and T. Sawara, The preliminary report of the third cruise for CSK, January to March 1969, *Oceanogr. Mag., 21,* 83–96, 1969.

Arthur, R. S., A review of the calculation of ocean currents at the equator, *Deep Sea Res., 6,* 287–297, 1960.

Austin, T. S., Variations with depth of oceanographic properties along the equator, *Eos Trans. AGU, 39,* 1055–1063, 1958.

Baker, D. J., and A. R. Robinson, A laboratory model for the general ocean circulation, *Phil. Trans. Roy. Soc. London, Ser. A, 265,* 533–566, 1969.

Bjerknes, J., 'El Nino' Study based on analysis of ocean surface temperatures, 1935–1957, *Bull. Inter-Amer. Trop. Tuna Comm., 5,* 219–303, 1961.

Bogdanov, C. H., and B. G. Popov, Currents of the surface layer of the western Pacific (in Russian), *Tr. Inst. Okeanol. Akad. Nauk SSSR, 40,* 135–142, 1960.

Bowden, F. P., and R. G. Lord, Aerodynamic resistance to a sphere rotating at high speed, *Proc. Roy. Soc. London, Ser. A, 271,* 143–153, 1963.

Brosin, H. J., and D. Nehring, Der Äquatoriale Unterstrom im Atlantischen Ozean auf 29°30'W im September und Dezember 1966, *Beitr. Meeresk., 22,* 5–17, 1968.

Bryan, K., and M. D. Cox, A non-linear model of an ocean driven by wind and differential heating, 1, 2, *J. Atmos. Sci., 25,* 945–978, 1968.

Buchanan, J. Y., On similarities in the physical geography of the great oceans, *Proc. Roy Geogr. Soc. London, 8,* 753–770, 1886.

Buchanan, J. Y., The exploration of the Gulf of Guinea, *Scot. Geogr. Mag., 4,* 177–200, 233–251, 1888.

Burkov, V. A., Water circulation in the North Pacific (in Russian), *Okeanologiya, 3,* 761–776, 1963.

Burkov, V. A., Structure and nomenclature of Pacific Ocean currents, *Oceanology, 6,* 3–14, 1966.

Burkov, V. A., and I. M. Ovchinnikov, Investigations of equatorial currents to the north of New Guinea (in Russian), *Tr. Inst. Okeanol. Akad. Nauk SSSR, 40,* 121–134, 1960.

Burkov, V. A., V. S. Arsentyev, and I. M. Ovchinnikov, Northern and southern tropical fronts in the ocean (in Russian), *Tr. Inst. Okeanol. Akad. Nauk SSSR, 40,* 108–120, 1960.

Carrier, G. F., Some effects of stratification and geometry in rotating fluids, *J. Fluid Mech., 23,* 145–172, 1965.

Charney, J. G., Non-linear theory of a wind-driven homogeneous layer near the equator, *Deep Sea Res., 6,* 303–310, 1960.

Charney, J. G., and S. L. Spiegel, The structure of wind-driven equatorial currents in homogeneous oceans, *J. Phys. Oceanogr., 1,* 149–160, 1971.

Christensen, N., Observations of the Cromwell Current near the Galapagos Islands, *Deep Sea Res., 18,* 27–34, 1971.

Cochrane, J. D., Equatorial Undercurrent and related currents off Brazil in March and April 1963, *Science, 142,* 669–671, 1963.

Cochrane, J. D., Equatorial currents of the Western Atlantic, Oceanography and Meteorology of the Gulf of Mexico, *Progr. Rep. 66-17T,* pp. 6–19, Dep. of Oceanogr. Meteorol., Texas A&M Univ., College Station, Tex., 1965.

Cochrane, J. D., Currents and waters of the western equatorial Atlantic, Oceanography of the Gulf of Mexico, *Prog. Rep. 66-23T,* pp. 28–32, Dep. of Oceanogr., Texas A&M Univ., College Station, Tex., 1966.

Colin, C., and H. Rotschi, Aspects géostrophiques de la circulation à l'équateur, *C.R.H. Acad. Sci., Ser. B, 271,* 929–932, 1971.

Colin, C., C. Henin, P. Hisard, and C. Oudot, Le Courant de Cromwell dans le Pacifique central en février, *Cah. Orstom, Ser. Oceanogr., 9,* 167–186, 1971.

Crease, J., and A. Pogson, Observations of the Equatorial Undercurrent by submarine, *Deep Sea Res., 11,* 391–393, 1964.

Cromwell, T., Circulation in a meridional plane in the central equatorial Pacific, *J. Mar. Res., 12,* 196–213, 1953.

Cromwell, T., and J. L. Reid, A study of oceanic fronts, *Tellus, 8,* 94–101, 1956.

Cromwell, T., R. B. Montgomery, and E. D. Stroup, Equatorial Undercurrent in the Pacific revealed by new methods, *Science, 119,* 648–649, 1954.

Defant, A., *Physical Oceanography,* vol. 2, pp. 556–591, Pergamon, New York, 1961.

Dowden, J. M., An equatorial boundary layer, *J. Fluid Mech., 56,* 193–200, 1972.

Düing, W., *The Monsoon Regime of the Currents in the Indian Ocean, Int. Indian Ocean Exped. Oceanogr. Monogr. Ser.,* vol. 1, p. 68, East-West Centre Press, Honolulu, 1969.

Felzenbaum, A. I., On the theory of steady wind-driven ocean circulation (in Russian), Lomonosov Current, *Publ. 34,* pp. 24–48, Moscow Hydrol. Inst., Ukr. Acad. Sci., Kiev, USSR, 1966.

Fofonoff, N. P., and R. B. Montgomery, The Equatorial Undercurrent in the light of the vorticity equation, *Tellus, 7,* 518–521, 1955.

Fuglister, F. C., *Atlantic Ocean Atlas,* vol. 1, Woods Hole Oceanogr. Inst., Woods Hole, Mass., 1960.

Gerard, R., R. Sexton, and P. Mazeika, Parachute drogue measurements in the eastern tropical Atlantic in September, 1964, *J. Geophys. Res., 70,* 5696–5698, 1965.

Gill, A. E., The Equatorial Current in a homogeneous ocean, *Deep Sea Res., 18,* 421–431, 1971.

Gill, A. E., Models of equatorial currents, paper presented at Symposium on Numerical Models of Ocean Circulation, Nat. Acad. Sci., Durham, N. H., Oct. 17–20, 1972.

Greenspan, H. P., *The Theory of Rotating Fluids,* p. 263, Cambridge University Press, New York, 1968.

Groves, G. W., Periodic variations of sea level induced by equatorial waves in the easterlies, *Deep Sea Res., 3,* 248–252, 1956.

Groves, G. W., and M. Miyata, On weather-induced long waves in the equatorial Pacific, *J. Mar. Res., 25,* 115–126, 1967.

Hidaka, K., Non-linear theory of an equatorial flow, with special application to the Cromwell Current, *J. Oceanogr. Soc. Jap., 20th Anniv. Vol.,* 223–241, 1962.

Hisard, P., and P. Rual, Courant Equatorial Intermediare de l'Ocean Pacifique et contre-courants adjacents, *Cah. Orstom, Ser. Oceanogr., 8,* 21–45, 1970.

Hisard, P., Y. Magnier, and B. Wauthy, Comparison of the hydrographic structure of equatorial waters north of New Guinea and at 170°E, *J. Mar. Res., 27,* 191–205, 1969.

Hisard, P., J. Merle, and B. Voituriez, The Equatorial Undercurrent at 170°E in March and April, 1967, *J. Mar. Sci., 28,* 281–303, 1970.

Holton, J. R., J. M. Wallace, and J. A. Young, On boundary layer dynamics and the I.T.C.Z., *J. Atmos. Sci., 28,* 275–280, 1971.

Ingham, M. C., and R. B. Elder, Oceanic conditions off northeast Brazil February–March and October–November 1966, *Rep. 34,* pp. 1–25, U.S. Coast Guard Oceanogr. Unit, Washington, D. C., Dec. 1970.

Istoshina, Yu. V., and A. A. Kalashnikov, The Cromwell Current in the western part of the Pacific, *Oceanology, 5,* 14–17, 1965.

Istoshin, Yu. V., and G. N. Kuklin, The Cromwell Current at 154°W (in Russian), *Okeanologiya, 2,* 262–263, 1962.

Ivanov, Yu. A., Hydrological researches in the northern part of the Indian Ocean (in Russian), *Tr. Inst. Okeanol. Akad. Nauk SSSR, 64,* 22–42, 1964.

Jones, J. H., Surfacing of Pacific Equatorial Undercurrent: Direct observation, *Science, 163,* 1449–1450, 1969.

Khanaychenko, H. K., N. Z. Khlystov, and V. G. Zhidkov, The system of equatorial countercurrents in the Atlantic Ocean, *Oceanology, 5,* 24–32, 1965.

Knauss, J. A., Measurements of the Cromwell Current, *Deep Sea Res., 6,* 265–286, 1960.

Knauss, J. A., On some aspects of the deep circulation of the Pacific, *J. Geophys. Res., 67,* 3943–3954, 1962.

Knauss, J. A., The Equatorial current systems, in *The Sea,* vol. 1, edited by M. N. Hill, pp. 235–252, Interscience, New York, 1963.

Knauss, J. A., Further measurements and observations on the Cromwell Current, *J. Mar. Res., 24,* 205–240, 1966.

Knauss, J. A., and J. E. King, Observations of Pacific Equatorial Undercurrent, *Nature, 182,* 601–602, 1958.

Knauss, J. A., and B. A. Taft, Measurements of currents along the equator in the Indian Ocean, *Nature, 198,* 376–377, 1963.

Knauss, J. A., and B. A. Taft, Equatorial Undercurrent of the Indian Ocean, *Science, 143,* 354–356, 1964.

Kolesnikov, A. G., G. P. Ponomarenko, N. K. Khanaychenko, and V. F. Shapkina, Subsurface Lomonosov Current (in Russian), in Lomonosov Current, *Publ. 34,* pp. 3–23, Moscow Hydrol. Inst., Ukr. Acad. Sci., Kiev, USSR, 1966.

Kolesnikov, A. G., S. G. Boguslavskiy, G. N. Kuklin, V. A. Shirey, and V. G. Kiryukhin, Lomonosov Current in the Gulf of Guinea, *Oceanology, 11,* 311–315, 1971.

Kort, V. G., V. A. Burkov, and K. A. Tchekotillo, New data on equatorial currents in the western Pacific (in Russian), *Dokl. Akad. Nauk SSSR, 171,* 337–339, 1966.

Koshlyakov, M. N., and V. G. Neyman, Some results of measurements and calculations of zonal currents in the Pacific equatorial region, *Oceanology, 5,* 37–49, 1965.

Kozlov, V. F., On the theory of a baroclinic layer at the equator, *Oceanology, 7,* 448–455, 1967.

Krivelevitch, L. M., A non-linear model of the flow of an inhomogeneous fluid at the equator, *Izv. Acad. Sci. USSR Atmos. Oceanic Phys., 4,* 105–110, 1968.

Leishman, C., Numerical methods for solving the non-linear problem of a wind-driven

homogeneous equatorial undercurrent, M.S. thesis, 42 pp., Dep. of Meteorology, Mass. Inst. Technol., Cambridge, Mass., 1967.

LeMasson, L., and B. Piton, Anomalie dynamique de la surface de la mer le long de l'équateur dans l'Océan Pacifique, *Cah. Orstom, Ser. Oceanogr., 6,* 39–46, 1968.

Masuzawa, J., An oceanographic section from Japan to New Guinea at 137°E in January 1967, *Oceanogr. Mag., 19,* 95–118, 1967.

Masuzawa, J., Second cruise for C.S.K., Ryofu Maru, January to March 1968, *Oceanogr. Mag., 20,* 173–185, 1968.

Masuzawa, J., The Mindanao Current (in Japanese), *Bull. Jap. Soc. Fish. Oceanogr.,* special number (Prof. Uda's Commem. Pap.), 99–104, 1969.

Masuzawa, J., T. Akiyama, Y. Kawarada, and T. Sawara, Preliminary reports of the Ryofu Maru Cruise RY7001 in January–March 1970, *Oceanogr. Mag., 22,* 1–25, 1970.

Matthäus, W., Zur Entdeckungsgeschichte des Äquatorialen Unterstrom im Atlantischen Ozean, *Beitr. Meeresk., 23,* 37–67, 1969.

McKee, W. D., The wind-driven equatorial circulation in a homogeneous ocean, *Deep Sea Res., 20,* in press, 1973.

Metcalf, W. G., Reply to comments by E. D. Stroup and R. B. Montgomery concerning the history of the Equatorial Undercurrent, *J. Geophys. Res., 68,* 343, 1963.

Metcalf, W. G., Shallow currents along the northeast coast of South America, *J. Mar. Res., 26,* 232–243, 1968.

Metcalf, W. G., and M. C. Stalcup, Origin of the Atlantic Equatorial Undercurrent, *J. Geophys. Res., 72,* 4959–4975, 1967.

Metcalf, W. G., A. D. Voorhis, and M. C. Stalcup, The Atlantic Equatorial Undercurrent, *J. Geophys. Res., 67,* 2499–2508, 1962.

Mintz, Y., and G. A. Dean, The observed mean field of motion of the atmosphere, *Geophys. Res. Pap., 17,* 11–65, 1952.

Montgomery, R. B., Equatorial Undercurrent observations in review, *J. Oceanogr. Soc. Jap., 20th Anniv. Vol.,* 487–498, 1962.

Montgomery, R. B., and E. Palmén, Contribution to the question of the Equatorial Countercurrent, *J. Mar. Res., 3,* 112–133, 1940.

Montgomery, R. B., and E. D. Stroup, Equatorial waters and currents at 150°W in July–August 1952, *Oceanogr. Study 1,* 68 pp., Johns Hopkins Univ., Baltimore, Md., 1962.

Moore, D. W., Equatorial Waves, paper presented at Symposium on Numerical Models of Ocean Circulation, Nat. Acad. Sci., Durham, N. H., Oct. 17–20, 1972.

Munk, W. H., On the wind-driven ocean circulation, *J. Meteorol., 7,* 79–93, 1950.

Neumann, G., Evidence for an equatorial undercurrent in the Atlantic Ocean, *Deep Sea Res., 6,* 328–334, 1960.

Neumann, G., The Equatorial Undercurrent in the Atlantic Ocean, in *Proceedings of the Symposium on Oceanography and Fisheries Resources of the Tropical Atlantic, Abidjan, C.I.,* pp. 33–44, Unesco, Paris, 1969.

Neumann, G., and R. E. Williams, Observations of the Equatorial Undercurrent in the Atlantic Ocean at 15°W during Equalant I, *J. Geophys. Res., 70,* 297–304, 1965.

Noel, J., and J. Merle, Analyse des courants superficiels et subsuperficiels équatoriaux durant une période de six jours à 170°E, *Cah. Oceanogr., 21,* 663–671, 1969.

Pearson, C. E., Numerical solutions for the time-dependent viscous flow between two rotating concentric spheres, *J. Fluid Mech., 28,* 323–336, 1967.

Philander, S. G. H., The equatorial dynamics of a shallow homogeneous ocean, *Geophys. Fluid Dyn., 2,* 219–245, 1971*a*.

Philander, S. G. H., On the flow properties of a fluid between concentric spheres, *J. Fluid Mech., 47,* 799–809, 1971*b*.

Philander, S. G. H., The equatorial dynamics of a deep homogeneous ocean, *Geophys. Fluid Dyn., 3,* 105–123, 1972.

Philander, S. G. H., The equatorial thermocline, *Deep Sea Res., 20,* 69–86, 1973.

Ponomarenko, G. P., On the 10th cruise of R/V Mikhail Lomonosov (in Russian), *Okeanologiya, 2,* 164–172, 1962.

Ponomarenko, G. P., The Lomonosov deep countercurrent on the equator in the Atlantic (in Russian), *Dokl. Akad. Nauk SSSR, 149,* 1178–1181, 1963.

Proudman, I., The almost rigid rotation of viscous fluid between concentric spheres, *J. Fluid Mech., 1,* 505–516, 1956.

Puls, C., Oberflächentemperaturen und Strömungsverhaltmisse des Äquatorial-guertels des Stillen Ozeans, *Arch. Seewarte, 18,* 1, 1895.

Pushistov, P. Yu., The planetary atmospheric boundary layer in the equatorial region, *Izv. Acad. Sci., USSR Atmos. Oceanic Phys., 6,* 321–325, 1970.

Reid, J. L., A transequatorial Atlantic oceanographic section in July 1963 compared with other Atlantic and Pacific sections, *J. Geophys. Res., 69,* 5205–5215, 1964.

Reid, J. L., Intermediate waters of the Pacific Ocean, *Oceanogr. Study 2,* 85 pp., Johns Hopkins Univ., Baltimore, Md., 1965.

Rinkel, M. O., Some features of relationships between the Atlantic Equatorial Undercurrent and its associated salinity core, in *Proceedings of the Symposium on Oceanography and Fisheries Resources of the Tropical Atlantic, Abidjan, C.I.,* pp. 193–212, Unesco, Paris, 1969.

Rinkel, M. O., P. Sund, and G. Neumann, The location of the termination area of the Equatorial Undercurrent in the Gulf of Guinea during Equalant III, *J. Geophys. Res., 71,* 3893–3981, 1966.

Robinson, A. R., The general thermal circulation in the equatorial regions, *Deep Sea Res., 6,* 311–317, 1960.

Robinson, A. R., An investigation into the wind as the cause of the Equatorial Undercurrent, *J. Mar. Res., 24,* 179–204, 1966.

Robinson, A. R., and P. Welander, Thermal circulation on a rotating sphere, with application to the oceanic thermocline, *J. Mar. Res., 21,* 25–38, 1963.

Rotschi, H., and B. Wauthy, Remarques sur le Courant de Cromwell, *Cah. Orstom, Ser. Oceanogr., 7,* 27–43, 1969.

Rual, P., Courants équatoriaux profonds, *Deep Sea Res., 16,* 387–391, 1969.

Seitz, R. C., Thermostad, the antonym of thermocline, *J. Mar. Res., 25,* 203, 1967.

Stalcup, M. C., and W. G. Metcalf, Direct measurements of the Atlantic Equatorial Undercurrent, *J. Mar. Res., 24,* 44–55, 1966.

Stalcup, M. C., and C. E. Parker, Drogue measurements of shallow currents on the equator in the western Atlantic Ocean, *Deep Sea Res., 12,* 535–536, 1965.

Stevenson, M. R., and B. A. Taft, New evidence of the Equatorial Undercurrent east of the Galapagos Islands, *J. Mar Res., 29,* 103–115, 1971.

Stewartson, K., On rotating laminar boundary layers, in *Boundary Layer Research: Grenzschiehtforschung I.U.T.A.M. Symposium—Freiburg, Aug. 26–29, 1957,* edited by H. Goertler, Springer, New York, 1958.

Stewartson, K., On almost rigid rotations, 2, *J. Fluid Mech., 26,* 131–144, 1966.

Stommel, H., The westward intensification of wind-driven ocean currents, *Eos Trans. AGU, 29,* 202–206, 1948.

Stommel, H., Wind-drift near the equator, *Deep Sea Res., 6,* 298–302, 1960.

Stone, P. H., The symmetric baroclinic instability of an equatorial current, *Geophys. Fluid Dyn., 2,* 147–164, 1971.

Stroup, E. D., The thermostad of the 13-C water in the equatorial Pacific Ocean, p. 202, Ph.D. dissertation, Johns Hopkins Univ., Baltimore, Md., 1969.

Stroup, E. D., and F. W. Hunt, Measurements of equatorial currents in the Gilbert Island area July–Aug. 1963, *Nature, 200,* 1001–1002, 1963.

Stroup, E. D., and R. B. Montgomery, Comments on the history of the Equatorial Undercurrent, *J. Geophys. Res., 68,* 341–342, 1963.

Sturm, M., and K. Voigt, Observations of the structure of the Equatorial Undercurrent in the Gulf of Guinea in 1964, *J. Geophys. Res., 71,* 3105–3108, 1966.

Swallow, J. C., Equatorial Undercurrent in western Indian Ocean, *Nature, 204,* 436–437, 1964.

Swallow, J. C., The Equatorial Undercurrent in the western Indian Ocean in 1964, Studies

in Tropical Oceanography, no. 5, pp. 15–36, Univ. of Miami Press, Coral Gables, Fla., 1967.

Taft, B., and J. Jones, Measurements of the Equatorial Undercurrent in the eastern Pacific, *Progr. Oceanogr., 6,* in press, 1973.

Taft, B., B. Hickey, C. Wunsch, and D. Baker, The Cromwell Current at 150°W, *Deep Sea Res., 20,* in press, 1973.

Taft, B. A., Equatorial Undercurrent of the Indian Ocean, 1963, Studies in Tropical Oceanography, no. 5, pp. 3–14, Univ. of Miami Press, Coral Gables, Fla., 1967.

Taft, B. A., and J. A. Knauss, The Equatorial Undercurrent of the Indian Ocean as observed by the Lusiad expedition, *Bull. Scripps Inst. Oceanogr., 9,* 1967.

Tsuchiya, M., An oceanographic description of the Equatorial Current system of the western Pacific, *Oceanogr. Mag., 13,* 1–30, 1961.

Tsuchiya, M., Upper waters of the intertropical Pacific Ocean, *Oceanogr. Study 4,* 50 pp., Johns Hopkins Univ., Baltimore, Md., 1968.

Veronis, G., An approximate analysis of the Equatorial Undercurrent, *Deep Sea Res., 6,* 318–327, 1960.

Voigt, K., Äquatoriale Unterstroming auch im Atlantic, *Beitr. Meeresk., 1,* 56–60, 1961.

Voigt, K., M. Sturm, F. Moeckel, and E. Benkelsdorff, Salinity, temperature, velocity profiles in the equatorial waters of the Gulf of Guinea areas, in *Proceedings of the Symposium on the Oceanography and Fisheries Resources of the Tropical Atlantic, Abidjan, C.I.,* pp. 179–184, Unesco, Paris, 1969.

Voit, S. S., and S. S. Strekalov, On the Lomonosov Current (in Russian), *Okeanologiya, 4,* 809–812, 1964.

von Schemainda, R., M. Sturm, and K. Voigt, Vorläufige Resultate der Untersuchungen im Bereich des äquatorialen Unterstroms im Golf von Guinea mit 'Professor Albrecht Penck' in der Zeit von April bis Juli 1964, *Beitr. Meeresk., 15,* 5–13, 1964.

White, W. B., The Equatorial Undercurrent, the South Equatorial Countercurrent, and their extensions in the South Pacific Ocean east of the Galapogos Islands during February–March 1967, *Rep. 69-4-T,* 74 pp., Texas A&M Univ., College Station, Tex., 1969.

Williams, R. G., An investigation of the intermediate salinity maximum in equatorial Atlantic during Equalant I, *Rep. GSL-TR 66-4,* 93 pp., Res. Div., N. Y. Univ., New York, 1966.

Wooster, W. S., Investigations of equatorial undercurrents, *Deep Sea Res., 6,* 263–264, 1960.

Wyrtki, K., Surface currents of the eastern tropical Pacific Ocean, *Bull. Inter-Amer. Trop. Tuna Comm., 9,* 271–304, 1965.

Wyrtki, K., Oceanography of the eastern equatorial Pacific Ocean, *Oceanogr. Mar. Biol. Rev., 4,* 33–68, 1966.

Wyrtki, K., and E. B. Bennett, Vertical eddy viscosity in the Pacific Equatorial Undercurrent, *Deep Sea Res., 10,* 449–455, 1963.

Wyrtki, K., and R. Kendall, Transports of the Pacific Equatorial Countercurrent, *J. Geophys. Res., 72,* 2073–2076, 1967.

Yamanaka, H., N. Anraku, and J. Morita, Seasonal and long-term variations in oceanographic conditions in the western North Pacific Ocean (in Japanese), *Rep. 22,* pp. 35–70, Nankai Reg. Fish. Res. Lab., Sanbashidori, Kochi, Japan, 1965.

Yosida, S., H. Nitani, and N. Suzuki, Report of multiple ship survey in the equatorial region (I.G.Y.) Jan.–Feb. 1958 (in Japanese), *Hydrogr. Bull. Tokyo, 59,* 1–30, 1959.

(Received February 28, 1973; revised April 13, 1973.)